



1 **Methods to homogenize ECC ozonesonde measurements across changes in  
2 sensing solution concentration or ozonesonde manufacturer**

3 Terry Deshler<sup>1</sup>, Rene Stübi<sup>2</sup>, Francis J. Schmidlin<sup>3</sup>, Jennifer L. Mercer<sup>1,7</sup>, Herman G. J. Smit<sup>4</sup>, Bryan J.  
4 Johnson<sup>5</sup>, Rigel Kivi<sup>6</sup>, and Bruno Nardi<sup>1,8</sup>

5

- 6 1. Department of Atmospheric Science, University of Wyoming, Laramie, Wyoming, USA
- 7 2. Meteo Swiss, Payerne, Switzerland
- 8 3. NASA Goddard Space Flight Center, Greenbelt, Maryland, USA
- 9 4. Forschungszentrum Jülich GmbH, Institute of Energy and Climate Research: Troposphere,  
Jülich, Germany.
- 10 5. Finnish Meteorological Institute, Arctic Research, Sodankylä, Finland.
- 11 6. National Oceanic and Atmospheric Administration, Boulder, Colorado, USA
- 12 7. Now at National Science Foundation, Geosciences Directorate, Division of Polar Programs,  
Arlington, Virginia, USA
- 13 8. Nardi Scientific, LLC, Denver, Colorado, USA

14  
15  
16 Correspondence to: T. Deshler ([deshler@uwyo.edu](mailto:deshler@uwyo.edu)).  
17  
18

19 **Abstract.**

20 From the mid 1990s to the late 2000s the consistency of electrochemical cell ozonesonde long term  
21 records has been compromised by differences in manufacturers, Science Pump and ENSCI, and  
22 differences in recommended sensor solution concentrations, 1.0% potassium iodide (KI) and the one  
23 half dilution 0.5%. To investigate these differences a number of organizations independently  
24 undertook comparisons of the various ozonesonde types and solution concentrations, resulting in 197  
25 ozonesonde comparison profiles. The goal is to derive transfer functions to allow measurements  
26 outside of standard recommendations, for sensor composition and ozonesonde type, to be converted to  
27 a standard measurement and thus homogenize the data to the expected accuracy of 5% (10%) in the  
28 stratosphere (troposphere). Subsets of these data have been analyzed previously and intermediate  
29 transfer functions derived. Here all the comparison data are analyzed to compare: 1) differences in  
30 sensor solution composition for a single ozonesonde type, 2) differences in ozonesonde type for a  
31 single sensor solution composition and 3) the World Meteorological Organization's (WMO) and  
32 manufacturer's recommendations of 1.0% KI solution for Science Pump and 0.5% KI for ENSCI.  
33 From the recommendations it is clear that ENSCI ozonesondes and 1.0% KI solution result in higher  
34 amounts of ozone sensed. The results indicate that differences in solution composition and in  
35 ozonesonde type display little pressure dependence at pressures  $\geq 30$  hPa and thus the transfer function  
36 can be characterized as a simple ratio of the less sensitive to the more sensitive method. This ratio is  
37 0.96 for both solution concentration and ozonesonde type. The ratios differ at pressures  $< 30$  hPa such  
38 that  $OZ_{0.5\%} / OZ_{1.0\%} = 0.90 + 0.041 \cdot \log_{10}(p)$  and  $OZ_{\text{SciencePump}} / OZ_{\text{ENSCI}} = 0.764 + 0.133 \cdot \log_{10}(p)$ .  
39 For the manufacturer recommended solution concentrations the dispersion of the ratio (SP-1.0/EN-  
40 0.5), while significant, is generally within 3% and centered near 1.0, such that no changes are  
41 recommended. For stations which have used multiple ozonesonde types with solution concentrations  
42 different from the WMO's and manufacturer's recommendations, this work suggests that a reasonably  
43 homogeneous data set can be created if the quantitative relationships specified above are applied to the  
44 non-standard measurements. This result is illustrated here in an application to the Nairobi data set.

45  
46



47 **1. Introduction**

48 Ozone is one of the critical atmospheric trace gases. Ozone contributes to the oxidizing capacity of  
49 the troposphere, to the absorption of terrestrial IR radiation, and to the absorption of solar UV in the  
50 stratosphere. An overabundance of ozone in the troposphere causes air quality problems, while a  
51 deficit in the stratosphere leads to enhanced exposure to UV. Ozone measurements are thus required to  
52 maintain our understanding of these processes and are required over times scales of hours to years, and  
53 from single point measurements to vertical profiles to the mid stratosphere. Measurements are required  
54 over hours at single locations to characterize air quality, while regular profiles over decades are  
55 required to characterize stratospheric ozone loss and to contribute to climate modeling.

56 Historically, the first ozone profile information was extracted from the Dobson measurements with  
57 the discovery of the Umkehr effect in the 1930s [Götz et al., 1934]. In optimal (blue sky) conditions at  
58 sunrise and at sunset two coarse resolution ( $\delta z \approx 7$  km) vertical ozone profiles from about 15 to 50 km  
59 could be retrieved by this technique and the first stratospheric ozone climatology created [Dobson et  
60 al., 1927]. Since this manual measurement method was demanding in personal resources it is only  
61 since the mid 1950s that continuous Umkehr measurements are available and the technique continues  
62 to be improved [Fioletov et al., 2006; Petropavlovskikh et al., 2005]. In the 1960s, wet-chemical  
63 ozonesondes were developed providing *in situ* high vertical resolution ( $\delta z \approx 0.3$  km or less) ozone  
64 profiles from the ground to the mid stratosphere [Brewer and Milford, 1960; Komhyr, 1965]. Datasets  
65 more than 30 years long are available based on this technique [Harris et al., 1998; Stähelin et al., 2001;  
66 Jeannet et al., 2007]. In the 1970s, the satellite epoch began providing global coverage of the total  
67 ozone column [e.g. Labow et al., 2013]. In the 1990s, the active lidar and the passive microwave were  
68 developed with an improved time resolution and an extended altitude range up to the mesosphere  
69 [Beekman et al., 1994; Calisesi et al., 2003; Moreira et al., 2015]. Today, the full suite of ground  
70 based, balloon-borne, and satellite instruments provide significant spatio-temporal coverage of global  
71 ozone. Maintaining this coverage requires all three platforms. Satellite instruments have limited life  
72 times and require comparison measurements with other instruments for algorithm development and  
73 reference measurements. Balloon-borne instruments provide the highest vertical resolution and the  
74 highest sensitivity but are limited in spatial and temporal coverage. Ground based instruments are  
75 required for long time series with single reference instruments and for daily measurement capability  
76 [e.g. Guirlet et al., 2000]. Modeling activities ranging from weather forecasts to climate studies benefit  
77 from ozone distribution measurements from all three platforms [Stein et al., 2000, Cionni et al., 2011].

78 Ozone is recognized as an Essential Climate Variable (ECV) and target observation requirements  
79 for satellite based products for climate are defined by the Global Climate Observing System (GCOS),  
80 which is a joint undertaking of the World Meteorological Organization (WMO), the United Nations  
81 Environmental Program, and others [GCOS, 2010]. The measurement requirements for an ECV  
82 represent a challenge even for ground based instruments:

- 83 1. Accuracy: 10% (troposphere), 5% (stratosphere).
- 84 2. Spatial resolution: Horizontal: 5-50 km (troposphere), 50-100 km (stratosphere).
- 85 3. Vertical resolution: 0.5 km (troposphere), 0.5-3 km (stratosphere).
- 86 4. Three hourly observing cycle everywhere.
- 87 5. Stability: 1 % (troposphere), 0.6% (stratosphere).

88 Since the late 1960s the vast majority of vertical ozone profile information is from individual  
89 ozonesonde flights. The instruments used are all based on measurements of an electrical current from  
90 an electrochemical galvanic cell which is a measure of the amount of ozone sampled. The current is  
91 generated when ozone in the air, which is bubbled through an electrolytic solution, reacts with iodide  
92 ions in the electrolyte in the cell. Variations of this principle, described in detail in section 2.1, led to  
93 the Brewer-Mast (BM) ozonesonde [Brewer and Milford, 1960], the Japanese KC ozonesonde  
94 [Komhyr and Harris, 1965; Kobayashi and Toyama, 1966], and the electrochemical concentration cell  
95 (ECC) ozonesonde [Komhyr, 1969]. The BM ozonesonde consists of a single electrochemical cell  
96 with a potential applied across the silver anode and platinum cathode immersed in an alkaline  
97 potassium iodide (KI) solution. The KC ozonesonde has a platinum cathode and carbon anode  
98 immersed in a pH neutral KI solution. The ECC ozonesonde consists of two half cells each containing  
99 a platinum electrode, and differing concentrations of iodide  $I^-$  in the form of KI, saturated at the anode



101 and dilute at the cathode. From these three electrochemical cell possibilities, the ECC ozonesonde has  
102 emerged as the preferred technology. One station continues using the BM ozonesonde for data  
103 continuity. The KC ozonesonde is no longer in use. Here we focus on the ECC ozonesonde.

104 While the ECC was under development different concentrations of KI in the cathode were  
105 investigated and the results compared with corresponding total column measurements. In the 1980s  
106 solution concentrations of 1.5 and 1.0% were in use [Barnes et al., 1985; Komhyr et al., 1995a]. By  
107 the mid 1980's a 1.0% solution of KI became the standard recommendation for Science Pump (SP)  
108 ozonesondes [Komhyr, 1986]. SP was the only manufacturer of ECC ozonesondes until the mid  
109 1990s, when the company ENSCI (EN) was formed, which began manufacturing an alternate ECC  
110 ozonesonde. Initially ENSCI also recommended a KI concentration of 1.0% for the cathode; however,  
111 this was changed to 0.5% after unpublished comparisons of EN and SP ozonesondes using 1.0% KI  
112 indicated that EN ozonesondes recorded more ozone than the SP ozonesondes at the same solution  
113 concentration.

114 These changes created some confusion as recommendations in the preparation of ECC  
115 ozonesondes changed. The first results comparing ozonesondes flown with 1.0% and 0.5% KI  
116 cathode solution were based on only a few comparisons [Boyd et al., 1998]. More extensive results  
117 were obtained from comprehensive intercomparisons in the laboratory [Smit et al., 2007], and in the  
118 field [Kivi et al. 2007; Deshler et al., 2008]. These comparisons led to the current WMO  
119 recommendations for ECC ozonesonde preparations [Smit and ASOPOS Panel, 2014]; however,  
120 between the mid 1990s and late 2000s the ozonesonde community was using several variations  
121 between 1.0% and 0.5% KI cathode cell concentrations in SP and EN ozonesondes. To homogenize  
122 these records to a single standard requires transfer functions to convert measurements made with any  
123 of the various combinations to one of the two WMO recommended standard preparations: 1.0% for SP  
124 and 0.5% for EN for the KI concentrations of the cathode electrolyte. Obtaining these transfer  
125 functions is the goal of this paper.

126 The transfer functions will be derived from published and unpublished measurements which  
127 compare directly the response of SP and EN ECC ozonesondes using 1.0 and 0.5% concentrations of  
128 KI in the cathode cells under identical environments of ozone, pressure, and temperature. These  
129 comparisons were done in an environmental simulation chamber in Jülich, Germany [Smit et al.,  
130 2007], henceforth JOSIE09, on a multiple ECC ozonesonde gondola [Deshler et al., 2008], henceforth  
131 the BESOS experiment, on other multiple ozonesonde balloon flights [Kivi et al., 2007], and on  
132 unpublished dual ozonesonde flights from Payerne, Switzerland; McMurdo Station, Antarctica;  
133 Sodankylä, Finland; Wallops Island, Virginia, USA; and Laramie, Wyoming, USA. Together 197  
134 comparisons of the different possible combinations have been made at these sites with the goal to  
135 develop transfer functions to convert measurements made with either manufacturer and with either 1.0  
136 or 0.5% KI concentration to one of the WMO recommendations: SP with 1.0% KI, EN with 0.5% KI.

137

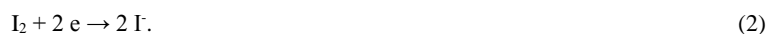
## 138 2. ECC ozonesonde description

### 139 2.1. ECC ozonesonde principles

140 Ozonesondes are based on an electrochemical cell where the chemical potential difference is  
141 maintained by differences in the iodide ( $I^-$ ) concentration in each half cell. Ozone introduced into the  
142 dilute iodide half reacts with iodide and converts it to iodine ( $I_2$ ) in the following reaction [Komhyr,  
143 1969]:



145 followed at the cathode by the reduction of iodine back to potassium iodide:



147 The two electrons arise from the electrolyte saturated in iodide at the anode by the oxidation of iodide:





149 The outer electrical circuit consists of two platinum electrodes immersed in the half cell  
150 electrolytes which are aqueous solutions of KI. The electrolyte is saturated with KI on the anode side  
151 and with a dilute KI concentration on the cathode side. Besides KI, the electrolytes also contain  
152 potassium bromine and sodium phosphate buffers to maintain a neutral pH solution. The  
153 decomposition of each ozone molecule in the dilute electrolyte produces a transfer of electrons (Eq. 2)  
154 in the outer circuit following Faraday's law of electrolysis. Converting the mass of ozone decomposed  
155 to partial pressure with the ideal gas law and substituting  $e \cdot N_A$  for Faraday's constant results in the  
156 following relationship between ozone partial pressure and electrical current:

$$157 \quad O_3(p) = \frac{R}{(z \cdot e \cdot N_A)} \cdot \frac{\phi(p)}{P_E(p)} \cdot \frac{T_p(p)}{FR} \cdot (i(p) - i_0). \quad (4)$$

158  $R$  is the universal gas constant,  $z$  the number of electrons required to convert the iodine in the dilute  
159 electrolyte back to iodide,  $e$  the elementary charge,  $N_A$  Avogadro's number,  $i(p)$  the measured cell  
160 current as a function of atmospheric pressure,  $p$ ,  $i_0$  the background current,  $\phi(p)$  the effective  
161 stoichiometry factor of the chemical conversion of ozone into iodine,  $T_p(p)$  the pump temperature, a  
162 surrogate for the temperature of the air sampled,  $FR$  the flow rate,  $P_E(p)$  the pump efficiency  
163 correction to account for decreasing flow rate at low pressures. Operationally, for  $i(p)$  in units of  $\mu\text{A}$ ,  $z$   
164 = 2, and  $FR$  in units of  $\text{ml s}^{-1}$ , the leading term in Eq. 4,  $R/(z e N_A)$  is replaced by  $4.3085 \times 10^{-6}$  which  
165 gives ozone partial pressure in  $\text{mPa}$ .

166 Each of the terms in Eq. 4 has an uncertainty deduced from the measurement method but they also  
167 have an additional uncertainty which is more difficult to quantify, especially at high altitude (low  
168 pressure) levels. The background current,  $i_0$ , the flowrate,  $FR$ , the pump temperature,  $T_p(p)$ , and the  
169 stoichiometry of ozone to iodine,  $\phi(p)$ , require special mention.

170 The back ground current  $i_0$  is a measure of the residual signal with "zero-air" (no ozone) at the  
171 ozonesonde inlet. Originally,  $i_0$  was attributed to side chemical reactions with oxygen and therefore,  
172 expected to decrease with altitude; however, Thornton and Niazy [1982] and Thornton [1983] and  
173 other empirical evidence from laboratory tests, suggested that  $i_0$  is constant independent of altitude.  
174 Figure 1 gives the range of  $i_0$  measured at the different stations prior to the measurement flights  
175 considered in this analysis. A mid value of  $0.03 \mu\text{A}$  from Figure 1 corresponds to  $0.1 \text{ mPa}$  and  
176 produces an offset of the ozone profile and a diminution of the ozone column by 5.4 DU,  $0.1 \text{ mPa}$   
177 integrated from  $1000 \text{ hPa}$  to  $1 \text{ hPa}$ , or 1.8% for a  $300 \text{ DU}$  ozone column. These  $i_0$  values will be  
178 discussed again in section 3.2, but the value of  $i_0$  does not affect comparisons between cells with  
179 similar backgrounds, and is thus less important for the work here.

180 The flow rate  $FR$  is well characterized in the laboratory preparation at surface pressure as shown  
181 in the box and whisker plot of the flow rates, Figure 2, measured at the different stations. The median  
182 values for each ozonesonde type are within  $0.3 \text{ ml s}^{-1}$ ,  $< 10\%$ , showing the good concordance between  
183 stations, although there is a  $0.2 \text{ ml s}^{-1}$  systematic difference between the majority of SP and EN  
184 ozonesondes. The real flow rate is much less certain at low pressure (high altitude) conditions where  
185 the pump efficiency decreases and pressure against the flow from the height of the solution in the ECC  
186 cell, on the order of  $1-2 \text{ hPa}$ , becomes non-negligible. Thus a pump efficiency correction is applied  
187 through the factor  $P_E(p)$ ; however, there is still disagreement on the correct  $P_E(p)$  to use [Johnson et  
188 al., 2002]. The pumps are designed for a constant rotation speed during a flight, a characteristic which  
189 has been checked by several investigators here but not published.

190 The effective stoichiometric factor,  $\phi(p)$  as formulated in Eq. 4, is composed of two factors: the  
191 absorption of ozone in the electrolytic solution, and the stoichiometric efficiency of the reaction of  $O_3$   
192 and KI to produce  $I_2$ . This latter factor is more difficult to characterize. In theory it is close to 1. The  
193 absorption efficiency has been measured in the laboratory with two ECC ozonesondes measuring in  
194 series. These tests have shown that the absorption of ozone is somewhat dependent on the amount of  
195 solution used (e.g.  $2.5 \text{ ml}$  vs.  $3.0 \text{ ml}$ ) [Tarasick et al., 2016; Davies et al., 2003], with the absorption  
196 increasing from 0.96 as the amount of solution increases from  $2.5 \text{ ml}$ . The increase of the gas diffusion  
197 rate during balloon ascent due to the pressure decrease should limit this ozone conversion efficiency  
198 loss to the lower part of the profile [Davies et al., 2003].



199 All these factors are eventually time and pressure dependent and they superpose each other which  
200 makes their individual contribution particularly difficult to determine. The factors which are of  
201 particular concern for the issue of varying ozonesonde manufacturer and cathode solution  
202 concentration are contained in the terms  $z$  and  $\varphi(p)$ . The details of the differences in ozonesonde  
203 manufacturer and how they affect these terms can only be speculated on at this time. The differences  
204 in cell manufacturer may affect the efficiency of electron release at the anode and electron gain by  
205 iodine at the cathode, or may affect reactions of ozone and the cell walls. Either of these would affect  
206  $z$ . Differences in KI concentration in the dilute electrolytic solution likely affects the efficiency of the  
207 conversion of  $O_3$  into  $I_2$  through reaction with KI, thus affecting  $\varphi(p)$ .

## 208 2.2. Review of the standard WMO recommendations

209 The preparation before the flight of an ECC ozonesonde is crucial for its performance. The  
210 Standard Operating Procedures (SOPs) for ECC ozonesondes have been established by a group of  
211 experts under the guidance of the World Calibration Center for Ozonesondes (WCCOS) of the WMO  
212 [Smit and the ASOPOS panel, 2014]. These results are from a ten year coordinated process to improve  
213 the different aspects of ECC ozonesonde preparation and data processing. Operating the ECC  
214 ozonesondes under these prescribed rules has been tested extensively in different JOSIE experiments  
215 at the Jülich Research Center [Smit et al., 2007]. The large balloon experiment BESOS was designed  
216 as an extension in the real atmosphere of these laboratory developments [Deshler et al., 2008]. In  
217 addition to 18 ozonesondes, the BESOS gondola included also the Jülich reference UV spectrometer  
218 [Proffitt et al., 1983, Smit et al., 2007] to replicate as far as possible the test procedure of the JOSIE  
219 experiments. The two experiments agree on the following conclusions:

- 220 1. ECC ozonesondes prepared according to the SOPs provide very reproducible (<2-3%)  
221 measurements.
- 222 2. The results depend on the ozonesonde manufacturer (e.g. EN vs. SP) and on the sensing  
223 solution concentration (e.g. 0.5% vs. 1.0%). The order of magnitude of the differences is  
224 5%.
- 225 3. The combinations "EN-0.5%" and "SP-1.0%" as "provider-solution" agree with each other  
226 to within 2%, but overestimate the reference UV photometer in the stratosphere by 5-10%.  
227 However, the total ozone column estimated from these combinations on the BESOS  
228 gondola agreed with a collocated Dobson spectrophotometer.
- 229 4. It is possible to reconcile the measurements made with other "provider-solution"  
230 combinations and the photometer with the help of a simple linear in  $\ln(p)$  transfer function.

231 JOSIE and BESOS were completed under conditions not reflecting directly the diversity of the  
232 operational services around the world. Each sounding station has specific instrumentation and  
233 operators even though they follow the same procedures. It is therefore important to verify that the  
234 conclusions from JOSIE and BESOS are also reflected in results of several operational stations. At the  
235 stations, it is not possible to fly a reference UV instrument so only relative differences can be derived  
236 from dual or multiple ozonesonde flights. In the present analysis the JOSIE and BESOS results will be  
237 analyzed in a similar way as the other dual multi instrument flights.

## 238 2.3. Review of previous solution concentration and provider comparisons

239 In the mid 1990s the problems of differences in "provider-solution" combinations were still of  
240 marginal importance [SPARC, 1998]. The EN-SCI company had entered the market only a few years  
241 earlier and the disparate preparation procedures prevented clearly identifying problems. The  
242 conclusions at that time were that the effect of changes in ECC KI solution concentrations were  
243 complex and required further study before clear recommendations could be provided.

244 McPeters et al. [1999] reports a 2% consistency from five triple ECC flights during a validation  
245 campaign at Mauna Loa in 1995 using EN 1.0% ozonesondes. The authors report that the ozonesondes  
246 overestimate the Dobson measurements by an average of 5%. In profile, above 25 km, the ozonesonde  
247 measurements are greater than the lidar and microwave measurements by a similar amount. Boyd et al.  
248 [1998] presented ozone profile differences from EN ozonesondes with 1.0 and 0.5% KI solutions at  
249 Lauder, New Zealand. A 5-6% systematic overestimation of ozone by the 1% solution compared to the  
250 0.5% with the EN ozonesondes is evidenced by comparison of the ozone profile and total column  
251 collocated lidar and Dobson measurements.



252 For an analysis of the transition from Brewer Mast to ECC (EN - 1.0%) ozonesondes, the ECC  
253 data were normalized to the Dobson column to be consistent with the Brewer Mast SOPs [Stübi et al.,  
254 2008]. Stübi et al. found that the ECC ozonesondes systematically overestimated the total ozone  
255 column with a mean normalization factor of 0.95 for more than 100 dual flights between ECC and BM  
256 indicating an overestimation of 5% of the ozone column by EN-1.0 ozonesondes.

257 Kivi et al. [2007] analyzed a series of dual and multiple ozonesonde flights with SP and EN  
258 instruments using 0.5% and 1.0% sensing solutions. For the homogenization of ozone profiles from  
259 the Northern high latitude stations the authors derived a third order polynomial correction based on  
260 altitude to correct the overestimation of ozone from EN-1.0% compared to SP-1.0%.

261 The laboratory work (Smit et al. [2007] along with the several field measurements (Boyd et al.  
262 [1998]; McPeters et al. [1999]; Stübi et al. [2008]; Kivi et al. [2007]; Deshler et al. [2008] all indicate  
263 a relatively consistent systematic bias, on the order of 5%, between the different ozonesonde  
264 manufacturers with the same electrolytic concentration, and between different electrolyte  
265 concentrations in ozonesondes from a single manufacturer.

#### 266 **2.4. Chemistry of the ECC ozonesonde**

267 The early stoichiometric work on the yield of iodine from ozone showed varying results with  
268 much of the uncertainty arising from the variety of KI sensing solutions, pH buffers, and sensors used  
269 [Saltzman and Gilbert, 1959; Boyd et al., 1970; Dietz et al., 1973; Pitts et al., 1976; Lanting, 1979].  
270 Common to many of the references was the suggestion of a secondary reaction producing additional  
271 iodine perhaps from reactions of iodide with the phosphate buffers. Johnson et al. [2002] showed that  
272 the same type of ECC ozonesonde operated with differing amounts of KI, and corresponding changes  
273 in the phosphate buffers, provide slightly different stoichiometric ratios of iodine to ozone. In fact  
274 these differences were very apparent in the initial development of the ECC ozonesondes [Komhyr,  
275 1969; 1986].

276 More difficult to identify are the reasons for the differences between the SP and EN ozonesondes  
277 which are in principle the same, yet the EN ozonesondes consistently indicate a higher ozone amount  
278 when compared to an SP ozonesonde with the same sensor KI electrolyte concentration. This may be  
279 related to differences in the platinum electrode sensitivity, the ion bridge conductance, or the inner  
280 surface properties of the cells. A detailed study of the reasons for the differences has not been  
281 performed and is beyond the scope of this paper. As will be shown the effect is very similar to the  
282 effect of differences in KI concentration.

#### 283 **2.5. Need for homogenization for data comparison**

284 The Montreal protocol signed in 1991 has established the publication every four years of an Ozone  
285 Assessment [e.g. WMO, 2010; 2014]. One of the most comprehensive reports regarding measurement  
286 techniques was the SPARC-IOC-GAW study [WMO, 1998]. An update of this study, the SI2N  
287 (SPARC/IGACO/IOC/NDACC) initiative to report the present state of knowledge of the different  
288 techniques and to reprocess long time series accordingly is being covered in a special issue of Atmos.  
289 Chem. Phys., Atmos. Meas. Tech., and ESSD. A parallel European Space Agency-CCI (Climate  
290 Change Initiative) project was established in 2011 to improve the satellites' products for the prominent  
291 "Essential Climate Variables", one being ozone. Comparisons with current satellite measurements of  
292 ozone, and future instrumental improvements for new satellite generations, require more accurate  
293 ground based data series for validation [Liu et al., 2006; Hubert et al., 2016]. Such comparisons have a  
294 rich heritage in previous field campaigns comparing various methods to measure ozone [Hilsenrath et  
295 al., 1986; Kerr et al., 1994; Margitan et al., 1995; Komhyr et al., 1995b; Meijer et al., 2004].

296 The MOZAIC datasets [e.g. Thouret et al., 1998; 2006] obtained from in-service aircraft provide a  
297 comparison to tropospheric ozonesonde measurements especially at the tropopause where ozone  
298 profiles are at their minimum values. Staufer et al. [2013; 2014] found a systematic difference with  
299 ozonesondes when aircraft measurements were compared to ozonesonde measurements determined by  
300 matching balloon and aircraft measurements via air parcel trajectory calculations, concluding an  
301 overestimation by the ozonesondes on the order of 5-10 % in the upper troposphere - lower  
302 stratosphere region. Logan et al. [2012] extensively analyzed tropospheric ozonesonde data by



303 comparison to MOZAIC aircrafts' ascent/descent profiles and to high altitude ground based  
304 measurements, pointing out biased and suspicious datasets.

305 Clear improvement of ozonesonde measurement precision for properly prepared and analyzed  
306 instruments is shown in recent comparison experiments for both the EN and SP instruments [Smit et  
307 al., 2007; Deshler et al., 2008]. A good sign of the stability of these results in the last ten years is  
308 confirmed in recent studies, e.g. Logan et al. [2012]. These results are not the case for the accuracy of  
309 measurements with "provider-solution" combinations which differ from the recommendations. Such  
310 combinations typically deviate from trusted ozone measurements by 5-10%. These latter deviations  
311 are now reasonably well characterized by a large set of comparison measurements, Table 1. Thus, it is  
312 time to apply corrections to ozonesonde data measured with provider-solution combinations differing  
313 from the standard WMO recommendations. Such applications will homogenize these data sets and  
314 thereby improve data quality, usefulness for trend analysis, global homogeneity, and references for  
315 satellites and models. The appropriate corrections to apply, using the large comparison data set  
316 available, are developed in sections 3 and 4.

### 317 **3. Methods to establish the transfer function**

#### 318 **3.1. Summary of datasets considered in the present analysis.**

319 The present analysis of dual ozonesonde measurements is an extension of the JOSIE and BESOS  
320 experiments to link short term instrument comparison campaigns to routine operations at regular  
321 sounding stations. JOSIE and BESOS used the same reference UV photometer [Proffitt et al., 1983]  
322 for the final comparisons and the results of those comparisons confirmed the high precisions and good  
323 accuracy of well-prepared ozonesondes. For the extensive additional data presented here an  
324 independent (e.g. photometric) reference is not available, rather the ozonesondes are compared  
325 pairwise. The JOSIE and BESOS data are included here also pairwise, Table 2. The first of these dual  
326 ozonesonde comparisons began in the late 1990s at different locations. Although there was no  
327 coordinated effort, the motivation at each station was similar. The need for homogenization of the long  
328 term ozonesonde record at the station. Table 1 summarizes the datasets used for the present analysis.  
329 Differences in the details of these comparisons at the different stations are described below.

##### 330 **3.1.1 JOSIE09 – Ozone profile simulation chamber, Jülich, Germany**

331 The JOSIE experiments have been described by Smit and Kley [1998], Smit and Sträter [2004a, b]  
332 and Smit et al. [2007] so only the experimental principles are reviewed here. Four ozonesondes can be  
333 placed simultaneously in the atmospheric simulator. Pressure and temperature can be regulated from  
334 surface conditions to 10 hPa and -70°C. The ozone flow is controlled in a glass cavity and measured in  
335 parallel by the ozonesondes and a reference UV photometer. Different types of "temperature-pressure-  
336 ozone" profiles are generated to simulate high-, middle- or tropical-latitude profiles. In the present  
337 analysis, only pairs of ozonesondes, representing different provider-solution combinations,  
338 simultaneously operated in the chamber are considered. This explains the low number of comparisons  
339 available for these data.

##### 340 **3.1.2. BESOS – Balloon-borne multi instrument gondola, Laramie, Wyoming**

341 The BESOS experiment was described fully by Deshler et al. [2008]. A collaborative team of  
342 ozonesonde experts prepared a balloon gondola (100 kg) with 16 ozonesondes, the Jülich UV  
343 photometer [Proffitt et al., 1983], a Vaisala radiosonde, and a data acquisition system. Dobson and  
344 Brewer spectrophotometers were available at the launch site. The flight to 32 km was completed on 13  
345 April 2004 from Laramie, Wyoming. The data from this flight are used here similarly to the JOSIE  
346 data by considering the ozonesondes pairwise. The payload had a set of 12 standard ozonesondes, 6  
347 from EN and 6 from SP; out of each set of 6 ozonesondes, 3 had a 0.5% and 3 a 1.0% KI solution  
348 concentration. Thus, a set of nine pairs are available for each "provider-solution" combination, Table  
349 2.

##### 350 **3.1.3. Payerne, Switzerland – Balloon-borne dual ozonesonde gondolas**

351 The Payerne station is run under the responsibility of MeteoSwiss and the radiosondes used were  
352 the SRS model from the Swiss company Meteolabor. SRS radiosondes are not capable of interfacing  
353 two ozonesondes, so for the dual flights two independent receiving systems were used. These were



354 synchronized at the time of the launch to better than one second and the sampling frequency was about  
355 7 seconds. For the analysis, the data are interpolated to a common time scale to avoid any problems  
356 related to a difference of the pressure readings from the two ozonesondes. The datasets consist in two  
357 campaigns embedded in the operational service as a dual flight for the Wednesday sounding. The  
358 reference (operational) ozonesonde being the EN-0.5%. The data sets consist of:  
359 1) 48 pairs EN-0.5% and EN-1.0% - June 2002 - July 2003.  
360 2) 26 pairs EN 0.5% and SP 1.0% - May 2005 - December 2006.

#### 361 **3.1.4. McMurdo Station, Antarctica – Balloon-borne dual ozonesonde gondolas**

362 Measurements from McMurdo Station, Antarctica, were conducted by the University of Wyoming  
363 during the ozone hole period, August –November, 1986-2010 [Mercer et al., 2007]. From this record  
364 18 flights with two EN ozonesondes interfaced to a single microprocessor and Vaisala RS80  
365 radiosonde were completed. The years (number of flights) are: 1996 (3), 1999 (1), 2000 (1), 2002 (6)  
366 and 2006 (7). In each case EN-1.0% and EN-0.5 % KI concentration solutions were compared. The  
367 low temperature conditions in Antarctica require a heater near the cells to prevent the solution freezing  
368 at high altitude. This preventive action is visible on Figure 3 with a mean pump temperature which  
369 stays close to 24°C at high altitude. The background currents are low with a slightly higher value for  
370 the ozonesondes with 1.0% solution compared to the 0.5%, Figure 1. This dataset is characterized by a  
371 large variety of ozone profiles from typical ozone hole to more conventional polar conditions; ozone  
372 column ranges are 126 - 423 DU.

#### 373 **3.1.5. Sodankylä, Finland – Balloon-borne dual and multi ozonesonde gondolas**

374 The Sodankylä station is run by the Finnish Meteorological Institute. The radiosondes used for  
375 the dual sonde and multiple sonde measurements were the Vaisala RS80. In the dataset used here there  
376 is a mix of 5 dual flights and 4 larger balloon flights with "6-sonde" payloads. The larger balloon  
377 payloads were recovered and flown again the next day with reused ozonesondes. The mean pump  
378 temperature profile shown in Figure 3 is characterized by the leveling of pump temperature at about  
379 22°C due to the use of a heater in case of the comparisons made under cold stratospheric conditions.  
380 For both the multiple and dual ozonesonde payloads a single RS80 radiosonde was applied per two  
381 ozonesondes, using interface extension boards provided by EN-SCI. Thus one receiving system was  
382 involved per two ozonesondes. The data set consists of

- 383 1) 6 pairs EN 0.5% and EN 1.0% - September 2003 - July 2004.
- 384 2) 5 pairs EN 0.5% and SP 1.0% - May 2003 - March 2005.
- 385 3) 8 pairs EN 1.0% and SP 1.0% - September 2003 - July 2004.

#### 386 **3.1.6. Wallops Island, Virginia - Balloon-borne dual ozonesonde gondolas**

387 Resources for ozonesonde measurements, with Sippican radiosondes, from Wallops Island have  
388 been, and continue to be, provided by NASA Headquarters. The Wallops Island practice is to use the  
389 background current measured during the day-of-flight preparation prior to exposing the ECC to  
390 moderate ozone (5 $\mu$ A) for 5 minutes; these backgrounds are smaller than the others shown in Figure 1.  
391 The values of  $i_o$  are, however, close to each other within the pairs so this difference has a negligible  
392 effect on the comparison measurements which were coordinated by matching the elapsed times of  
393 flight of the two systems, similar to the procedure for Payerne. The data sets consist of:

- 394 1) 7 pairs SP 5A-ECC's 0.5% vs. 1.0% in 1996.
- 395 2) 11 pairs SP 6A-ECC's 0.5% vs. 1.0% in 2004.

#### 396 **3.1.7 Laramie, Wyoming – Balloon-borne multi ozonesonde gondola**

397 These results were obtained from a collaboration between the Climate Monitoring and Diagnostic  
398 Laboratory (CMDL) of the National Oceanic and Atmospheric Administration and the University of  
399 Wyoming. CMDL prepared the gondola and the University of Wyoming conducted the flight  
400 operation. The measurements were obtained from a gondola containing 6 EN ozonesondes, 3 with  
401 0.5% KI and 3 with 1.0% KI. The instruments were synchronized to a common data system and an  
402 RS80 Vaisala radiosonde. The flight occurred on 20 June 1996 and reached an altitude of 32 km.

403

#### 404 **3.2. Data Processing**



405 The ozone data processing from the measured current is based on Eq. 4 with little variability  
406 among the datasets. The major difference is in the sampling frequency of the measurements which  
407 ranged from 0.2 to 1.0 Hz. The typical e-folding response of an ozonesonde is of the order of 0.05 Hz  
408 [Smit and Kley, 1998]. All the sampling rates here are faster than this, but are the same for every  
409 pairwise comparison so the sampling rate will not affect a comparison. However, since the data  
410 analysis is based on the individual pair differences, it is necessary to average the high frequency  
411 measurements to a common time scale to avoid unduly weighting the high frequency data relative to  
412 the lower frequency measurements. Ultimately the high frequency data were averaged to a frequency  
413 of 0.2 Hz so that when the data weighted means of the comparisons were calculated each comparison  
414 profile was weighted about equally.

415 **3.2.1. Back ground current  $i_0$**

416 In Figure 1, the background currents measured for the different data sets are summarized as box  
417 and whisker plots. For all sites except Wallops Island, these are the background currents after  
418 exposure to moderate ozone and just prior to flight. The  $i_0$  used at Wallops Island was prior to  
419 exposure to moderate ozone on the day of flight preparations. This may explain the slightly lower  
420 backgrounds obtained at Wallops Island. The medians of  $i_0$  from the various sites are all below 0.03  
421  $\mu\text{A}$  indicating the quality and consistency of the ozonesonde preparations. The  $i_0$  values for the 1.0%  
422 solution tend to be slightly higher compared to the 0.5% solution suggesting the impact of the larger  
423 buffer amount [Johnson et al., 2002]. Boyd et al. [1998] argue that the large difference between their  
424 ascent and descent ozone (tropospheric) profiles is attributable to an increase in the background  
425 current after exposure to high ozone in the stratosphere. They have observed this increase with the 1%  
426 solution but not with the 0.5%. Similarly in the laboratory preparation, the ozonesondes are exposed to  
427 high ozone for ten minutes and the slightly higher  $i_0$  values for the 1.0% solution could be related to  
428 such a memory effect. The origin of the background current is still poorly understood [Smit et al.,  
429 2007]. Vömel and Diaz [2010] measured the rate at which ozonesondes approach background in the  
430 laboratory, with some implications for measurements in the tropics of very low tropospheric ozone  
431 concentrations.

432 **3.2.2. Pump flow rate**

433 The pump flow rate is the second parameter measured in the laboratory preparation of each  
434 ozonesonde. Figure 2 shows the coherency of the pump flow rates at the 5 field measurements sites. In  
435 about half the measurement sets, the inner quartiles of the variations amongst the instruments  
436 measured are less than 3% of the median, and in all cases except one the inner quartiles are less than  
437 6% of the median. The figure also shows a systematically 0.2–0.3  $\text{ml s}^{-1}$  higher flow rate for SP pumps  
438 compared to EN pumps.

439 **3.2.3. Pump efficiency correction**

440 The application of pump efficiency corrections vary amongst the datasets. In general Komhyr  
441 [1986] is used for SP and Komhyr et al. [1995a] is used for EN ozonesondes. Since the comparisons  
442 analyzed are amongst pairs of identical ozonesondes, the pump efficiency does not play an important  
443 factor unless significantly different pump efficiencies were applied separately to the ozonesondes in a  
444 measurement pair. In most cases the same efficiency factors were applied to both ozonesondes of a  
445 pair. The one exception is the Wallops Island data, where individual pump efficiency curves were  
446 applied prior to mid 2000 when the system failed. The pairwise comparisons of these data, however,  
447 were quite similar to the Wallops Island data where identical pump efficiencies were used, and to the  
448 pairwise comparisons from the other data sets.

449 **3.2.4. Pump temperature**

450 For the data processing, individual pump temperatures are used as illustrated in Figure 3 for the  
451 mean pump temperature profiles for each dataset. The standard deviations of the temperature range  
452 from 1°C for McMurdo Station to 5°C for Sodankylä. The pump temperature decrease over a profile is  
453 around 7–10°C for the ozonesondes with a heater and 20–23°C for the ozonesondes without a heater.  
454 This parameter also is reproducible within the ozonesondes pairs and thus doesn't impact significantly  
455 the pairwise comparisons.



456

457 **4. Comparisons of ozone partial pressure**

458 In Figure 4, an example of a dual flight from Payerne is illustrated. The two ozonesondes  
459 separated by a 1.5 m long boom were hanging under the same balloon and the data transmitted to two  
460 independent receiving systems on the ground. The ozone profiles have identical structures and  
461 differences increase near the ozone maximum at pressures less than 50 hPa, indicating some  
462 dependence on both ozone partial pressure and atmospheric pressure. The increased sensitivity of the  
463 1.0% solution is clear throughout the profile.

464 **4.1. Differences between 1.0% and 0.5% KI cathode solutions for EN and SP ozonesondes**

465 The simplest way to analyze the data is to compare ozone partial pressures measured by  
466 ozonesonde pairs operated simultaneously, either in the atmosphere or in the simulation chamber.  
467 Scatter-plots of ozone partial pressure measured with ECC ozonesondes with 1.0% solution, x-axis,  
468 against simultaneous measurements with a 0.5% solution, y-axis, are shown in Figure 5 for EN  
469 ozonesondes flown from a) Payerne and b) McMurdo Station, and SP ozonesondes from c) BESOS  
470 and d) JOSIE09. The color coding distinguishes four pressure ranges to highlight the altitude  
471 (pressure) dependence. Only ozone partial pressures  $> 0.5\text{ mPa}$  have been considered to remove large  
472 differences resulting from comparisons of small numbers near the measurement limit of the  
473 ozonesondes. Figure 5 demonstrates a near linear relationship between the 0.5 and 1.0% ozonesonde  
474 measurements in the four pressure ranges considered, independent of the ozonesonde manufacturer.  
475 The mean and standard deviation of the measurement ratios in the various pressure intervals are given  
476 in the legends. The mean ratios are used to construct linear fits, which pass through the origin, to the  
477 measurements in each pressure range and are displayed in the Figure. The mean ratios and standard  
478 deviations for all the measurements from JOSIE09, BESOS, Payerne, and McMurdo Station at the  
479 four pressure intervals are given in Table 2. Table 2 also contains bulk fits to all data from Sodankylä,  
480 Wallops Island, and Laramie without differentiation according to pressure. Figure 5 and Table 2,  
481 upper two boxes, display the remarkable consistency amongst all the data from the varied sources.  
482 Note the consistency of the mean ratios and their standard deviations from all data sources. Figure 5  
483 and Table 2 also indicate a consistent 3-4% underestimation of ozone from a 0.5% KI solution  
484 compared to a 1.0% solution from the ground up to 30 hPa for both SP and EN ozonesondes. An  
485 increase of the difference to 6-8% at pressures below 30 hPa is also shown by the four data sets,  
486 Figure 5.

487 Table 2 also shows additional analysis in three other comparison groups: the third and fourth  
488 boxes correspond to a change of provider keeping the same concentration and the final box a fit to a  
489 mix of SP 1.0% and EN 0.5%. The tendency of a decrease of the linear term at lower pressures is  
490 present in most data sets except for this last group where the linear fit is not statistically different than  
491 the fits at pressures above 30 hPa. The correlation coefficients for the data are all above 0.9. There are  
492 four cases in Table 2, two in the Payerne and two in the BESOS datasets, with standard deviations  $>$   
493 0.1. These are all in the column for pressures  $> 500\text{ hPa}$ . The origin of the large standard deviations for  
494 Payerne, EN-1.0 vs EN-0.5, probably lies in the outliers apparent in Figure 5a) at pressures  $> 500\text{ hPa}$ .  
495 Such discrepancies are less obvious in the other Payerne comparison and in the BESOS data. The  
496 cause of these larger standard deviations was not investigated further in light of small standard  
497 deviations in all datasets at pressures less than 500 hPa.

498 Considering the strong linear relationship of the dual measurements for the differences in  
499 concentration in the same ozonesonde type, and differences in ozonesonde type with the same sensor  
500 concentration, it is natural to simply use a single ratio to characterize the relationship of the two  
501 measurements at pressures above a certain threshold pressure, and then to use a linear relationship in  
502  $\log_{10}(p)$  to fit the ratio at lower pressures, insuring that the two systems merge at the threshold  
503 pressure. The ratio of the measurements from a single manufacturer at two cathode concentrations is  
504 illustrated in Figure 6 as an ensemble of red dots for the same data sets as in Figure 5. The dual flight  
505 measurements at Payerne and McMurdo Station, Figure 6a), 6b), show a larger spread of the data but  
506 the number of measurements are considerably larger and the atmospheric conditions more diverse than  
507 in the BESOS and JOSIE experiments, Figure 6c), 6d). Occasionally, individual flights from Payerne  
508 and McMurdo Station deviate from the majority of comparisons, seen as a set of points separated from



509 the main cloud of points. These few comparisons are clear outliers compared to the majority of  
 510 measurements.

511 These comparisons suggest that measurements from ozonesondes using a 1.0% KI concentration  
 512 in the cathode can be used to derive measurements which would have been obtained from  
 513 measurements with a 0.5% KI solution if the measurements using the 1.0% KI solution are modified  
 514 using a pressure independent ratio at pressures above some threshold pressure and a pressure  
 515 dependent ratio below the threshold pressure. Different values for the threshold pressure to switch  
 516 from a single ratio to a pressure dependent ratio were tested but the results were not very sensitive to  
 517 this value and it has been fixed at 30 hPa.

518 With the threshold pressure level established each data set was used to calculate a mean  
 519 concentration ratio at pressures,  $p \geq 30$  hPa and a linear, in  $\log_{10}(p)$ , fit at  $p < 30$  hPa. The results of  
 520 this analysis are displayed in the upper two boxes of Table 3 for all datasets listed in Table 1. The  
 521 second column provides the concentration ratio and its standard deviation for  $p \geq 30$  hPa, the third  
 522 column the number of individual ozonesonde to ozonesonde comparisons (N). Recall each dataset was  
 523 standardized to a sampling frequency of 0.2 Hz to balance the weights of the high frequency and low  
 524 frequency data equally. Thus the number of data points represents primarily the number of individual  
 525 ozonesonde to ozonesonde comparisons within each dataset. For  $p < 30$  hPa columns 4, 5, and 6 list  
 526 the fitting parameters providing the slope in  $\log_{10}(p)$  and then the offset, corresponding to the value of  
 527 the concentration ratio at 1 hPa. Two offsets are listed. The first is the one used. The second offset is  
 528 derived without a requirement to match the  $p \geq 30$  hPa transfer function. The small differences  
 529 between these two offsets reflects the fact that the function chosen is doing a good job of representing  
 530 the data even without a fitting constraint. Column 7 provides the number of data points (N) at  $p < 30$   
 531 hPa, column 8 the number of dual ozonesonde measurements.

532 The coefficients for the transfer function representing the ratio of ozone sensed at the differing  
 533 concentrations were calculated as a weighted mean (according to sample size) of the individual  
 534 parameters given in Table 3 for all datasets considered in the analysis. These values comprise the final  
 535 row in each box in Table 3. Not all data from each dataset were used due to unstable ratios at  
 536 particularly low ozone concentrations, or during clearly deficient ozonesonde performance. The  
 537 primary examples of the data excluded are displayed as the dark areas in Figure 6. These data were  
 538 excluded for the following specific reasons:

- 539 1. McMurdo Station : Some of the dual measurements were completed in ozone hole  
 540 conditions, and in these cases ozone drops to near zero producing highly divergent ratios,
- 541 2. JOSIE: At three points during the simulated profiles, the ozone flow was stopped to  
 542 measure the residual signal and the response time, producing very low ozone and thus  
 543 likewise ratio divergences.
- 544 3. BESOS: in the first minutes of the flight, the data acquisition unit was unstable and too  
 545 noisy to consider in the present analysis.

546 The common transfer function to analyze differences in KI concentration,  $OZ_{conc}$ , is given in Eq. 5  
 547 and presented in Figure 6 as a blue line for  $p \geq 30$  hPa and a black line for  $p < 30$  hPa. The function  
 548 displayed in Eq. 5 accounts for a change of solution concentration independently of the ozonesonde  
 549 provider.

$$550 \frac{OZ_{0.5\%}(p)}{OZ_{1.0\%}(p)} = 0.96, \quad \text{for } p \geq 30 \text{ hPa}, \quad (5)$$

$$551 \frac{OZ_{0.5\%}(p)}{OZ_{1.0\%}(p)} = 0.90 + 0.041 \bullet \log_{10}(p), \quad \text{for } p < 30 \text{ hPa}.$$

552

#### 553 4.2. Difference between EN and SP with the same solution concentration

554 In Figure 7, profiles of the ratio of SP and EN ozonesondes with the same KI solution  
 555 concentration are shown in the same format as Figure 6. The upper panels show the difference  
 556 between the SP and EN ozonesondes with a 1.0% solution concentration while the lower panels are for



557 the 0.5% solution concentration. Figure 7a) is from multiple dual flights at Sodankylä over the period  
 558 1995-2002 while the other panels present the analysis of the JOSIE and BESOS experiments. Using  
 559 these data, and following the procedure used to reconcile the two solution concentrations in the same  
 560 ozonesonde provider, section 4.1, the common transfer function to correct a change from one provider  
 561 to the other was derived. Similar to the analysis in section 4.1 the results from fits to each data set and  
 562 their weighted mean are provided in the third and fourth box in Table 3. Combining the results from  
 563 the boxes comparing EN and SP ozonesondes at 1.0% and EN and SP ozonesondes at 0.5% results in  
 564 the transfer function,  $OZ_{prov}$ , given in Eq. 6.

565 
$$\frac{OZ_{SP}(p)}{OZ_{EN}(p)} = 0.96, \quad \text{for } p \geq 30 \text{ hPa} \quad (6)$$

566 
$$\frac{OZ_{SP}(p)}{OZ_{EN}(p)} = 0.764 + 0.133 \bullet \log_{10}(p), \quad \text{for } p < 30 \text{ hPa}$$

567 As for  $OZ_{conc}$ , the coefficients of the transfer function  $OZ_{prov}$  were calculated individually for the  
 568 five data sets and an overall mean, weighted by the number of comparisons and flights, calculated.  
 569 The JOSIE data present a larger spread than in the previous case and individual simulator runs are  
 570 visible. Aside from the BESOS data for 0.5% KI at  $p > 150$  hPa, Figure 7d), where there is a  
 571 tropospheric bias of 2%, the  $OZ_{prov}$  curve reproduces the results from the different data sets. The  
 572  $\log_{10}(p)$  coefficient is slightly larger in  $OZ_{prov}$  than in  $OZ_{conc}$  producing a lower value for the constant  
 573 term (intercept at 1 hPa) since the constant ratio terms are the same ( $\text{ratio}(OZ_{conc}) = \text{ratio}(OZ_{prov}) =$   
 574 0.96) for the  $p \geq 30$  hPa domain, while the decrease in the ozone ratio between the providers increases  
 575 at lower pressures comparable to the decrease in ozone ratio at differing solution concentrations,  
 576 Figure 6.

577

#### 578 4.3. Similarity between the combinations EN-0.5% and SP-1.0%

579 With the similarity of the two transfer functions  $OZ_{conc}$  and  $OZ_{prov}$ , it is natural to counterbalance  
 580 them and compare EN ozonesondes with 0.5% solution and SP ozonesondes with 1.0% solution. The  
 581 results are given in Figure 8 for a) Payerne, b) Sodankylä, c) BESOS, and d) JOSIE09. The horizontal  
 582 axis of Figure 8 is expanded compared to Figures 6 and 7 and the number of comparisons are low for  
 583 JOSIE (3 cases) and Sodankylä (5 cases). The agreement between the ozonesonde pairs is not as clear  
 584 as for the previous cases as illustrated by the Payerne data which present a somewhat larger dispersion  
 585 (10%) in Figure 8 compared to Figure 5 (5%). The BESOS data have a distinct behavior below and  
 586 above the tropopause (200 hPa) while the five Sodankylä flights show a constant 3% overestimations  
 587 by the SP ozonesondes. However, if no simple transfer function would allow to reconcile these  
 588 observations, it is noticeable that the majority of the points are within 3% around 1.0 illustrated by the  
 589 gray zone in Figure 8. Table 3 last 3 lines also reveal no marked departure from unity.

590 The present conclusion is that the interchange between the EN-0.5% and SP-1.0% combinations  
 591 would not have a negative impact on the continuity of a time series. It may increase the variability, but  
 592 no noticeable break should appear at the transition between these two systems.

593

#### 594 4.4. Transfer function application on the Nairobi data set

595 The Kenyan Meteorological Department (KMD), in collaboration with MeteoSwiss, operates the  
 596 Nairobi aerological station, within the SHADOZ (Southern Hemisphere ADDitional OZone station)  
 597 network, [Thompson et al., 2012]. Weekly ozone soundings began in 1996. In summer 2010, due to  
 598 interruption of the Vaisala RS80 radiosonde production, new equipment based on the RS92 was  
 599 installed at Nairobi. Coincidentally, the ozonesonde solution concentration was changed from 1.0% to  
 600 0.5%, keeping the same ozonesonde provider, EN. This data set is used here to illustrate the  
 601 application of the transfer function  $OZ_{conc}$  defined in Eq. 5. In Figure 9, a time series on three pressure  
 602 levels is illustrated. Color separates the measurements with the different solution concentrations. In the  
 603 troposphere, the ozone partial pressure is low (2.5 mPa) and the variability is too high to detect



604 changes of a few percent. Therefore the 500 hPa data illustrated in Figure 9 do not show the change of  
605 sensor concentration. At 30 hPa, the quasi biennial oscillation is the dominant signal and this requires  
606 at least a complete cycle after the change to correctly see the effect; however, there is a clear decrease  
607 of the mean ozone value before and after the change of concentration. Finally at 10 hPa, the lower  
608 variability and the absence of geophysical cycles in the data allow the effect of the concentration  
609 change to be clearly seen.

610 To quantify the concentration change, the mean ozone profiles before and after 2010 have been  
611 calculated and appear in Figure 10, with black squares for 1996 to 2010 and blue circles after 2010.  
612 Red triangles correspond to the 1996 - 2010 data after correction of each profile with the transfer  
613 function  $OZ_{conc}$ . The difference profiles are illustrated on the right side of Figure 10 in black for the  
614 original data and in red for the corrected data for the period 1996 - 2010. The error bars combine the  
615 variabilities of the two original mean profiles. Even though the differences were not significant for the  
616 pressure  $>30$  hPa, the correction shows a net improvement for the higher levels.

617 For a total ozone column comparison three estimations are available for Nairobi station: the  
618 ozonesonde integrated profile, a Dobson D018 co-located spectrophotometer and the OMI (Ozone  
619 Monitoring Instrument) satellite overpass measurements. The change of sensing solution and the  
620 corrections shown in Figure 10 have affected the ratios of the total column ozone as shown in Table 4.

621  
622 **5. Discussion**

623 There has been a significant effort to reconcile ozonesonde measurements completed with  
624 instruments from the two ozonesonde providers, Science Pump and ENSCI, with various combinations  
625 of the recommendations for the KI sensor solution concentrations 1.0% and 0.5%. The motivation for  
626 this effort rests on characterizations of the precision and accuracy achievable with well-prepared  
627 ozonesondes through laboratory tests [Smit and Sträter, 2004a; 2004b; Smit et al., 2007] and field tests  
628 [Logan et al., 1999; 2012; Kivi et al., 2007; Deshler et al., 2008]. These results have shown that the  
629 precision of an ECC ozonesonde is better than observed systematic differences between ozonesonde  
630 type or solution concentration. The results presented here demonstrate that the differences in  
631 ozonesonde type, with the same solution concentration, are quite systematic and thus can be  
632 characterized, to within experimental uncertainties, with a single relationship for both 0.5 and 1.0% KI  
633 concentrations. Similarly, systematic differences between sensor solution concentrations in the same  
634 ozonesonde for both SP and EN ozonesondes can also be characterized by a single relationship. These  
635 results attest to the consistency in ozonesonde manufacturing for both companies and that both  
636 ozonesonde types have similar differences in performance when the KI solution concentration is  
637 varied, pointing again to the strength of the instrumental technique and the instruments.

638 The rationale employed in this analysis was to find a simple set of relationships which could be  
639 applied throughout all the data analyzed. Clearly there are differences in the various datasets as shown  
640 in Figure 6. In this case the recommended relationship, Eq. 5, for the relationship between 0.5% and  
641 1.0% KI does not optimally fit the BESOS SP data, Figure 6c), but it does quite well against the  
642 Payerne and McMurdo Station data, Figure 6a), 6b). The overestimation of the BESOS SP data is  
643 counterbalanced by the under estimation of the JOSIE09 SP data, Figure 6d). This relationship does  
644 well against the BESOS EN 0.5 – 1.0% and the Wallops Island SP 0.5-1.0% comparisons (not shown).  
645 The relationship is not steep enough for the Sodankylä measurements at pressures  $< 30$  hPa.  
646 Differences such as these led to the alternate transfer functions using first to third order polynomials in  
647 log pressure derived by Kivi et al. [2007] and Deshler et al. [2008]. Neither of these relationships,  
648 however, would do well across the full data set analyzed here. In particular the third order polynomial  
649 provided by Kivi et al. was required due to the significant ratio decrease at pressures below 50 hPa.

650 Similar comments may arise from the analysis of the ozonesonde type comparisons, Figure 7,  
651 although in general the proposed relationship requiring a more significant decrease in the ozonesonde  
652 type ratio at pressures below 30 hPa is better at reproducing the ozonesonde type comparisons. The  
653 only dataset not shown in this comparison is from JOSIE09 comparing the ozonesonde types at 1.0%.  
654 That ratio profile compared to the relationships recommended is quite similar to the comparison at  
655 0.5%, Figure 7c).



656 The reasons behind the increase in ozone sensed with increase in KI concentration has not been  
657 fully explored and is beyond the scope of this paper. The discussions of this effect have centered on  
658 the importance of the sodium phosphate hydrate buffers used to maintain the pH of the solution. These  
659 buffers, which vary in proportion to the KI concentration, may lead to secondary reactions between  
660 iodide ions and the buffer leading to excess iodine, thus indicating additional ozone [Saltzman and  
661 Gilbert, 1959; Johnson et al., 2002]. Similarly there have been discussions on the reasons behind the  
662 increased sensitivity of the EN ozonesondes compared to SP ozonesondes. Speculation has centered  
663 on the efficiencies of the platinum electrode in scavenging the iodine, the conductance of the ion  
664 bridge, or the surface properties of the SP Teflon cells versus the EN molded plastic cells, but there  
665 has been no systematic investigation of this effect. This also remains beyond the scope of the work  
666 presented here.

667 For a transfer function to have wide acceptance within the community it must have reasonable  
668 application to the widest possible set of comparisons. Specialized transfer functions have been derived  
669 for particular subsets of the data [Kivi et al., 2007; Deshler et al., 2008] but it has not been  
670 demonstrated that these functions are useful beyond the specific data from which they were derived.  
671 The analysis here sought to develop as simple a relationship as possible based on the full comparison  
672 data set available. This was achieved through weighting of the ratio fits by the number of profile  
673 comparisons to arrive at the final four relationships described in Eqs. 5 and 6. Once derived the  
674 individual datasets were compared against the derived transfer functions and a subset of these shown  
675 in Figures 6 and 7. While Kivi et al. [2007] did not show such a comparison, Deshler et al. [2008] did.  
676 Figure 5 from Deshler et al. could be compared here against Figures 6c), 7b), and 7d). Compared to  
677 Deshler et al. the fits proposed here improve the comparisons of ozonesonde type while not  
678 significantly diminishing the comparisons of sensor concentration. Coupling this with the ability of the  
679 fits to reproduce nearly all data sets within the uncertainty of the fits provide strong support for the  
680 validity of the proposed transfer functions. This is not to argue that the relationships proposed here  
681 should be used instead of results of an individual investigation of a particular comparison dataset;  
682 however, such an individual transfer function must be supported by the appropriate measurement set,  
683 and made available publicly through the refereed literature. For investigators without access to the  
684 resources to conduct such a study, the transfer functions proposed here will do an adequate job of data  
685 homogenization.

686 The final comparison investigated here is between the two manufacturer's recommendations. This  
687 was done through 43 comparison profiles summarized in Figure 8. There was no attempt to derive a  
688 fitting function for these data and as the figure illustrates such an exercise would be difficult. The ratio  
689 of SP-1.0 to EN-0.5 has a wide dispersion, which is amplified in the figure by the reduced axes for the  
690 ratios, from 0.8 – 1.2 compared to Figures 6 and 7. Figure 8 suggests some bias in the smaller datasets  
691 investigated, with ratios  $> 1$  for Sodankylä and BESOS, but  $< 1$  for JOSIE09, while Payerne, by far  
692 the largest dataset, shows no systematic bias. The objective analysis shown in Tables 2 and 3 quantify  
693 these differences but also show that the differences are on average generally not different than 1.0 in  
694 contrast for the results of the solution concentration and ozonesonde type comparisons. Thus the data  
695 here suggest that the two, manufacturer and WMO, recommended ozonesonde type and solution  
696 concentration packages can be used directly and should be widely comparable.

697  
698 **6. Summary and Conclusions**

699 Measurements with various combinations of ozonesonde type, Science Pump or ENSCI, and with  
700 differing combinations of the KI solution concentration, 1.0% or 0.5%, have led to variations in  
701 ozonesonde preparation at a number of ozonesonde stations throughout the world. These changes  
702 began in the mid 1990s and played a role in the analysis of ozonesonde data between then and the late  
703 2000s [Mercer et al., 2007; Tarasick et al., 2016]. Recognizing that these differences exceeded the  
704 accuracy and precision that is possible from ozonesondes [Smit et al., 2007; Deshler et al., 2008] led  
705 many investigators to independently explore the differences that occur when the same ozonesonde is  
706 operated with differing solution concentrations, and when differing ozonesonde types are operated  
707 with the same solution concentrations [Johnson et al., 2002; Kivi et al., 2007; Smit et al., 2007;  
708 Deshler et al., 2008]. Measurements from these investigators and other unpublished comparisons have  
709 been analyzed in this paper. The analysis has focused on three basic comparisons: 1) Sensor solution



710 composition differences in ozonesondes of the same type, 2) Ozonesonde type differences using the  
711 same sensor solution concentration, and 3) Differences of the manufacturer and WMO  
712 recommendations, Science Pump 1.0% and ENSCI 0.5% KI solution concentrations. Using the  
713 published and unpublished data has resulted in the analysis here of 116 profile comparisons for  
714 solution concentration differences, 38 profile comparisons for ozonesonde type differences, and 43  
715 profile comparisons of the manufacturer's solution concentration recommendations. The datasets used  
716 in the comparisons have been obtained from the laboratory (JOSIE09), multi-sonde balloon-borne  
717 gondolas (BESOS, Sodankylä), and dual ozonesonde balloon-borne gondolas (Payerne, McMurdo  
718 Station, Sodankylä, Wallops I, Laramie), involving at least 6 different scientific groups.

719 Overall the measurements display a satisfying coherence when solution concentrations or  
720 ozonesonde type are compared. At pressures above 30 hPa, the surface to 30 hPa, the two  
721 measurements can be characterized with a simple ratio displaying almost no pressure dependence. In  
722 addition this ratio is, within experimental uncertainty, the same, 0.96, whether the difference is in  
723 solution concentration with the same ozonesonde type, or ozonesonde type with the same solution  
724 concentration. Ozone concentrations are higher for 1.0% versus 0.5% KI and for ENSCI compared to  
725 Science Pump ozonesondes. At pressures below 30 hPa there is a pressure dependence which is linear  
726 in  $\log_{10}$  of pressure. This pressure dependence is more pronounced for differences in ozonesonde type.  
727 The results arrived at here are simpler than previous recommendations, but are based on a much more  
728 comprehensive dataset and include all of the data used in deriving the previous transfer functions [Kivi  
729 et al., 2007; Deshler et al., 2008] both of whom arrived at a relationship requiring a polynomial in  
730 altitude or log of the pressure for all pressures. As evidenced here, when the full datasets are  
731 investigated, the complexity of these relationships is not justified by the data.

732 The conclusions arrived at from the analysis described here are the following:

733 For differences in solution concentration independent of ozonesonde type:

$$OZ_{0.5\%} = 0.96 \bullet OZ_{1.0\%}, \text{ for } p \geq 30 \text{ hPa},$$

$$OZ_{0.5\%} = [0.90 + 0.041 \bullet \log_{10}(p)] \bullet OZ_{1.0\%}, \text{ for } p < 30 \text{ hPa}.$$

736 For differences in ozonesonde type independent of solution concentration:

$$OZ_{\text{SciencePump}} = 0.96 \bullet OZ_{\text{ENSCI}}, \text{ for } p \geq 30 \text{ hPa},$$

$$OZ_{\text{SciencePump}} = [0.764 + 0.133 \bullet \log_{10}(p)] \bullet OZ_{\text{ENSCI}}, \text{ for } p < 30 \text{ hPa}.$$

739 We recommend that all ozonesonde measurements completed with 1.0% KI in ENSCI  
740 ozonesondes or 0.5% KI in Science Pump ozonesondes should adjust their data according to the  
741 relationships shown above such that the final data product would be representative of 0.5% KI ENSCI  
742 or 1.0% Science Pump. This should be done for any data prepared for analysis and for public  
743 availability. The investigation of 43 profiles comparing 1.0% KI in Science Pump ozonesondes and  
744 0.5% KI in ENSCI ozonesondes found that the dispersion in the comparisons was centered on a ratio  
745 of 1.0. Thus there is no recommendation to alter data obtained from instruments using the  
746 recommended concentrations.

747 If these recommendations are followed it can be expected that datasets experiencing variations in  
748 the use of ozonesonde type and solution concentration will see their long term data converge to within  
749 the expected  $\pm 5\%$  for ozonesondes, and that offsets at the times of transition between the ozonesonde  
750 type, or solution concentration change, or both, will be minimized. This will improve significantly the  
751 reliability of long term ozone measurements derived from ozone soundings, and indirectly stabilize, in  
752 space and time, the long term series of ozone measurements obtained from satellites.

753 These recommendations have been implemented in the WMO/Global Atmospheric Watch  
754 (GAW)'s guidelines for the homogenization of ozonesonde data [Smit and O3S-DQA-Panel, 2012],  
755 recommended to the ozone sounding stations of the Network for the Detection of Atmospheric  
756 Composition Change (NDACC) and to SHADOZ stations. The effort for the ozonesonde investigators  
757 to accomplish these corrections will be significant, but in the end the health of the network is  
758 dependent on such quality control measures being implemented, and it will greatly add to the value of  
759 the measurements. All future measurements should use the WMO/GAW recommendations for



760 solution composition. Any deviation from these recommendations should be justified and carefully  
761 researched prior to a change.

762 **Author contributions.** T. Deshler with R. Stübi performed the data analysis. T. Deshler was  
763 responsible for the majority of the writing with input from all co-authors. R. Stübi provided the  
764 Payerne data, F. J. Schmidlin the Wallops Island data, J. L. Mercer, B. Nardi the McMurdo Station  
765 data, H. G. J. Smit the JOSIE09 data, B. J. Johnson, the Laramie data, R. Kivi the Sodankylä data, T.  
766 Deshler the BESOS data.

767 **Data Availability.** The ozonesonde measurements used in this analysis are available from the  
768 individual investigators and the majority of these data are on the NDACC data base. These data and  
769 the code used to created Figures 4-8 are also compiled at  
770 [ftp://cat.uwyo.edu/pub/permanent/balloon/Manuscripts/Oz\\_Transfer\\_Functions/](ftp://cat.uwyo.edu/pub/permanent/balloon/Manuscripts/Oz_Transfer_Functions/). The data for Figures  
771 9 and 10 are available at the NDACC and SHADOZ data bases.

772 **Acknowledgments.** This work was encouraged by the ozonesonde working groups of the  
773 WMO/GAW, NDACC, and SHADOZ. The following agencies have supported the generation of these  
774 data sets: MeteoSwiss, Finnish Meteorological Institute, World Ozonesonde Calibration Facility, US  
775 National Science Foundation, US National Aeronautics and Space Administration, US National  
776 Oceanic and Atmospheric Administration.

## 777 References

778 Barnes, R. A., A. R. Bandy, and A. L. Torres: Electrochemical concentration cell ozonesonde  
779 accuracy and precision. *J. Geophys. Res.*, 90:7881-7887, 1985.  
780 Beekmann, M., G. Ancellet, G. Megie, H. Smit, and D. Kley: Intercomparison campaign for vertical  
781 ozone profiles including electrochemical sondes of ECC and Brewer-Mast type and a ground  
782 based UV-differential absorption lidar, *J. Atmos. Chem.*, 19, 259-288, 1994.  
783 Boyd, A. W., C. Willis, and R. Cyr: New determination of stoichiometry of the iodometric method for  
784 ozone analysis at pH 7.0, *Anal. Chem.*, 42, 670-672, 1970.  
785 Boyd, I., G. Bodeker, B. Connor, D. Swart, and E. Brinksma: An assessment of ECC ozondesondes  
786 operated using 1% and 0.5% KI cathode solutions at Lauder, New Zealand, *Geophys. Res. Lett.*,  
787 25, 2409-2412, 1998.  
788 Brewer, A. W., and J. R. Milford: The Oxford-Kew ozondesonde, *Proc. R. Soc. Lond. A.*, 256, 470-  
789 495, 1960.  
790 Calisesi, Y., R. Stübi, N. Kämpfer, and P. Viatte: Investigation of systematic uncertainty in Brewer-  
791 Mast ozone soundings using observations from a ground-based microwave radiometer, *J. Atmos.  
792 Ocean. Technol.*, 20, 1543-1551, 2003.  
793 Cionni, I., Eyring, V., Lamarque, J. F., Randel, W. J., Stevenson, D. S., Wu, F., Bodeker, G. E.,  
794 Shepherd, T. G., Shindell, D. T., and Waugh, D. W.: Ozone database in support of CMIP5  
795 simulations: results and corresponding radiative forcing, *Atmos. Chem. Phys.*, 11, 11267-11292,  
796 doi:10.5194/acp-11-11267-2011, 2011.  
797 Davies, J., McElroy, C. T., Tarasick, D. W., and Wardle, D. I.: Ozone Capture Efficiency in ECC  
798 Ozonesondes; Measurements made in the Laboratory and during Balloon Flights, EAE03-A-  
799 13703, Geophysical Research Abstracts, Vol. 5, 13703, EGS-AGU-EUG Joint Assembly, Nice,  
800 France, 6-11 April 2003.  
801 Deshler, T., J. Mercer, H. G. Smit, S. J. Oltmans, B. J. Johnson, R. Stübi, G. Levrat, J. Davies, A.  
802 Thompson, J. Witte, F. Schmidlin, G. B. Brothers, S. Toru, and M. Proffitt: Atmospheric  
803 comparison of electrochemical cell ozonesondes from different manufacturers, and with different  
804 cathode solution strengths: The Balloon Experiment on Standards for Ozonesondes, *J. Geophys.  
805 Res.*, 113, D04307, doi: 10.1029/2007JD008975, 2008.  
806 Dietz, R. N., J. Pruzansky, and J. D. Smith: Effect of pH on the stoichiometry of the iodometric  
807 determination of ozone, *Anal. Chem.*, 45, 402-404, 1973.  
808 Dobson, G.M.B., D.N. Harrison, and J. Lawrence: Measurements of the Amount of Ozone in the  
809 Earth's Atmosphere and Its Relation to Other Geophysical Conditions, Part II, *Proc. Roy. Soc. A*,  
810 114, 521-541, 1927.



812 Fioletov, V., D. Tarasick, and I. Petropavlovskikh: Estimating ozone vari-ability and instruments  
813 uncertainties from sbuv(2), ozonesondes, umkehr, and sage ii measurements: Short-term  
814 variations, *J. Geophys. Res.*, **111**, D02305, doi: 10.1029/2005JD006340, 2006.  
815 GCOS: Implementation Plan for the Global Climate Observing System (GCOS) in Support of the  
816 UNFCCC (2010 Update), GCOS-138 (GOOS-184, GTOS-76), World Meteorological  
817 Organization, Geneva, Switzerland, 2010.  
818 Götz, F. W. P., A. R. Meetham, and G. M. B. Dobson: The vertical distribution of ozone in the  
819 atmosphere, *Proc. Roy. Soc. A* **145**, 416.  
820 Guirlet, M., P. Keckhut, S. Godin, and G. Megie: Description of the long-term ozone data series  
821 obtained from different instrumental techniques at a single location: The Observatory de Haute-  
822 Provence (43.9°N, 5.7°E), *Ann. Geophys.*, **18**, 1325-1339, 2000.  
823 Harris, N., R. Hudson, and C. Phillips: Assessment of trends in the vertical distribution of ozone, in  
824 SPARC Rep. 1 and WMO Ozone Res. Monit. Proj. Rep. 43, World Climate Research Program,  
825 Geneva, Switzerland, 1998.  
826 Hilsenrath, E., R. Hagemeyer, J. Mentall, A. Torres, W. Attmannspacher, A. Bass, W. Evans, R. A.  
827 Barnes, W. Komhyr, and D. Robbins: Results from the Balloon Ozone Intercomparison Campaign  
828 (BOIC), *J. Geophys. Res.*, **91**, 13,137{13,152, 1986.  
829 Hubert, D., Lambert, J.-C., Verhoelst, T., Granville, J., Keppens, A., Baray, J.-L., Bourassa, A. E.,  
830 Cortesi, U., Degenstein, D. A., Froidevaux, L., Godin-Beckmann, S., Hoppel, K. W., Johnson, B.  
831 J., Kyrölä, E., Leblanc, T., Lichtenberg, G., Marchand, M., McElroy, C. T., Murtagh, D., Nakane,  
832 H., Portafaix, T., Querel, R., Russell III, J. M., Salvador, J., Smit, H. G. J., Stebel, K., Steinbrecht,  
833 W., Strawbridge, K. B., Stübi, R., Swart, D. P. J., Taha, G., Tarasick, D. W., Thompson, A. M.,  
834 Urban, J., van Gijsel, J. A. E., Van Malderen, R., von der Gathen, P., Walker, K. A., Wolfram, E.,  
835 and Zawodny, J. M.: Ground-based assessment of the bias and long-term stability of 14 limb and  
836 occultation ozone profile data records, *Atmos. Meas. Tech.*, **9**, 2497-2534, doi:10.5194/amt-9-  
837 2497-2016, 2016.  
838 Jeannet, P., R. Stübi, G. Levrat, P. Viatte, and J. Stähelin: Ozone balloon soundings at Payerne  
839 (Switzerland): re-evaluation of the time series 1967 - 2002 and trend analysis, *J. Geophys. Res.*,  
840 **112**, D11302, doi: 10.1029/2005JD006862, 2007.  
841 Johnson, B. J., S. J. Oltmans, H. Vömel, H. G. J. Smit, T. Deshler, and C. Kroger: Electrochemical  
842 concentration cell (ECC) ozonesonde pump efficiency measurements and tests on the sensitivity to  
843 ozone of buffered and unbuffered ECC sensor cathode solutions, *J. Geophys. Res.*, **107**, 4393,  
844 10.1029/2001JD000557, 2002.  
845 Kerr, J. B., H. Fast, C. McElroy, S. J. Oltmans, J. A. Lathrop, E. Kyrö, A. Paukkunen, H. Claude, U.  
846 Köhler, C. Sreedharan, T. Takao, and Y. Tsukagoshi: The 1991 WMO International  
847 Ozondesondes Intercomparison at Vanscoy, Canada, *J. Atmos. Ocean. Technol.*, **32**, 685-716,  
848 1994.  
849 Kivi, R., E. Kyrö, T. Turunen, N. R. P. Harris, P. von der Gathen, M. Rex, S. B. Andersen, and I.  
850 Wohltmann: Ozonesonde observations in the Arctic during 1989?2003: Ozone variability and  
851 trends in the lower stratosphere and free troposphere, *J. Geophys. Res.*, **112**, D08306, doi:  
852 10.1029/2006JD007271, 2007.  
853 Kobayashi, J. and Y. Toyama: On various methods of measuring the vertical distribution of  
854 atmospheric ozone (III) - Carbon iodine type chemical ozonesonde-. *Pap. Met. Geophys.*, **17**, 113-  
855 126  
856 Komhyr, W. D.: Operations handbook-ozone measurements to 40-km altitude with model 4A  
857 electrochemical concentration cell (ECC) ozonesondes (used with 1680-MHz radiosondes), in  
858 Technical memorandum ERL ARL-149, NOAA, Boulder, Colorado, 49pp, 1986.  
859 Komhyr, W. D.: Electrochemical concentration cells for gas analysis, *Ann. Geophys.*, **25** (1), 203-210,  
860 1969.  
861 Komhyr, W. D., and T. B. Harris: Note on flow rate measurements made on Mast-Brewer ozone  
862 sensor pumps, *Mon. Weather Rev.*, **93** (4), 267-268, 1965.  
863 Komhyr, W. D., R. A. Barnes, G. B. Brothers, J. A. Lathrop, and D. P. Opperman: Electrochemical  
864 concentration cell ozonesondes performance evaluation during STOIC 1989, *J. Geophys. Res.*,  
865 **100** (D5), 9231-9244, 1995a.



866 Komhyr, W.D., B. Connor, I. Mcdermid, T. McGee, A. Parrish, and J. Margitan: Comparison of  
867 STOIC 1989 ground-based lidar, microwave spectrometer, and Dobson spectrophotometer umkehr  
868 ozone profiles with ozone profiles from balloon-borne electrochemical concentration cell  
869 ozonesondes, *J. Geophys. Res.*, 100 (D5), 9273-9282, 1995b.

870 Labow, G. J., R. D. McPeters, P. K. Bhartia, and N. Kramarova: A comparison of 40 years of SBUV  
871 measurements of column ozone with data from the Dobson/Brewer network, *J. Geophys. Res.*  
872 *Atmos.*, 118, 7370–7378, doi:10.1002/jgrd.50503, 2013.

873 Lanting, R. W.: Modification of the potassium iodide procedure for improved stoichiometry, *Atmos.*  
874 *Environ.*, 13, 553– 554, 1979.

875 Liu, X., K. Chance, C. E. Sioris, T. P. Kurosu, and M. J. Newchurch: Intercomparison of GOME,  
876 ozonesonde, and SAGE II measurements of ozone: Demonstration of the need to homogenize  
877 available ozonesonde data sets, *J. Geophys. Res.*, 111 (D10), 14,305+, doi:  
878 10.1029/2005JD006718, 2006.

879 Logan, J. A., I. A. Megretskaya, A. J. Miller, G. C. Tiao, D. Choi, L. Zhang, R. S. Stolarski, G. J.  
880 Labow, S. M. Hollandsworth, G. E. Bodeker, H. Claude, D. D. Muer, J. B. Kerr, D. W. Tarasick,  
881 S. J. Oltmans, B. Johnson, F. Schmidlin, J. Staehelin, P. Viatte, and O. Uchino: Trends in the  
882 vertical distribution of ozone: a comparison of two analyses of ozonesonde data, *J. Geophys. Res.*,  
883 104 (D21), 26,373-26,399, 1999.

884 Logan, J.A., J. Staehelin, I. A. Megretskaya, J.-P. Cammas, V. Thouret, H. Claude, H. De Backer, M.  
885 Steinbacher, H.-E. Scheel, R. Stubi, M. Fröhlich, and R. Derwent: Changes in ozone over Europe:  
886 Analysis of ozone measurements from sondes, regular aircraft (MOZAIC) and alpine surface sites.  
887 *J. Geophys. Res. Atmos.*, 117, D09301, doi:10.1029/2011JD016952, 2012.

888 Margitan, J. J., R. A. Barnes, G. B. Brothers, J. Butler, J. Burris, B. J. Connor, R. A. Fer-rare, J. B.  
889 Kerr, W. D. Komhyr, M. P. McCormick, I. S. McDermid, C. T. McElroy, T. J. McGee, A. J.  
890 Miller, M. Owens, A. D. Parrish, C. L. Parsons, A. L. Torres, J. J. Tsou, T. D. Walsh, and D.  
891 Whiteman: Stratospheric ozone intercomparison campaign (STOIC) 1989: Overview, *J. Geophys.*  
892 *Res.*, 100, 9193-9208, doi: 10.1029/95JD00509, 1995.

893 McPeters, R. D., D. J. Hofmann, M. Clark, L. Flynn, L. Froidevaux, M. Gross, B. Johnson, G. Koenig,  
894 X. Liu, S. McDermid, T. McGee, F. Murcay, M. J. Newchurch, S. Oltmans, A. Parrish, R.  
895 Schnell, U. Singh, J. J. Tsou, T. Walsh, and J. M. Zawodny: Results from the 1995 Stratospheric  
896 Ozone Profile Intercomparison at Mauna Loa, *J. Geophys. Res.*, 104, 23, pp. 30505-30514, 1999.

897 Meijs, Y. J., D. P. J. Swart, M. Allaart, S. B. Andersen, G. Bodeker, I. Boyd, G. Braa-then, Y.  
898 Calisesi, H. Claude, V. Dorokhov, P. von der Gathen, M. Gil, S. Godin-Beekmann, F. Goutail, G.  
899 Hansen, A. Karpetchko, P. Keckhut, H. M. Kelder, R. Koele-meijer, B. Kois, R. M. Koopman, G.  
900 Kopp, J.-C. Lambert, T. Leblanc, I. S. Mc-Dermid, S. Pal, H. Schets, R. Stübi, T. Suortti, G.  
901 Visconti, and M. Yela: Pole-to-pole validation of Envisat GOMOS ozone profiles using data from  
902 ground-based and balloon sonde measurements, *J. Geophys. Res.*, 109 (D18), 23,305, doi:  
903 10.1029/2004JD004834, 2004.

904 Mercer, J. L., C. Kroger, B. Nardi, B. J. Johnson, M. P. Chipperfield, S. W. Wood, S. E. Nichol, M. L.  
905 Santee, and T. Deshler: Comparison of measured and modeled ozone above McMurdo Station,  
906 Antarctica, 1989-2003, during austral winter/spring, *J. Geophys. Res.*, 112,  
907 D19307, doi:10.1029/2006JD007982, 2007.

908 Moreira, L., Hocke, K., Eckert, E., von Clarmann, T., and Kämpfer, N.: Trend analysis of the  
909 20-year time series of stratospheric ozone profiles observed by the GROMOS microwave  
910 radiometer at Bern, *Atmos. Chem. Phys.*, 15, 10999-11009, doi:10.5194/acp-15-10999-  
911 2015, 2015.

912 Petropavlovskikh, I., P. K. Bhartia, and J. DeLuisi: New Umkehr ozone profile retrieval algorithm  
913 optimized for climatological studies, *Geophys. Res. Lett.*, 32, L16808,  
914 doi:10.1029/2005GL023323, 2005.

915 Pitts, J. N., Jr., J. M. McAfee, W. D. Long, and A. M. Winer: Long-path infrared spectroscopic  
916 investigation at ambient concentrations of the 2% neutral buffered potassium iodide method for  
917 determination of ozone, *Environ. Sci. Technol.*, 10, 787– 793, 1976.

918 Proffitt, M. H., and R. J. McLaughlin: Fast dual-beam uv-absorption photometer suitable for use on  
919 stratospheric balloons, *Rev. Sci. Instrum.*, 54, 1719-1728, 1983.



920 Saltzman, B. E., and N. Gilbert: Iodometric microdetermination of organic oxidants and ozone,  
921 resolution of mixtures by kinetic colorimetry, *Anal. Chem.*, 31, 1914– 1920, 1959.

922 Smit, H.G.J., and D. Kley: The 1996 WMO international intercomparison of ozonesondes under quasi  
923 flight conditions in the environmental simulation chamber at Jülich, in WMO Global Atmospheric  
924 Watch Report, 130, World Meteorological Organization, Geneva, 1998.

925 Smit, H.G.J., and W. Sträter: JOSIE-1998 performance of the ECC ozondesondes of SP-6A and  
926 ENSCI-Z type, in WMO Global Atmospheric Watch Report, 157, World Meteorological  
927 Organization, Geneva, 2004a.

928 Smit, H.G.J., and W. Sträter: The 2000 WMO international intercomparison of operating procedures  
929 for ECC-ozondesondes at the environmental simulation facility at Jülich, in WMO Global  
930 Atmospheric Watch Report, 158, World Meteorological Organization, Geneva, 2004b.

931 Smit, H. G. J., W. Sträter, B. J. Johnson, S. J. Oltmans, J. Davies, B. Hoegger, R. Stübi, F. Schmidlin,  
932 J. Witte, A. Thompson, I. Boyd, and F. Poisny: Assessment of the performance of ECC-  
933 ozondesondes under quasi-flight conditions in the environmental simulation chamber: Insights  
934 from the Jülich Ozondesonde Intercomparison Experiment (JOSIE), *J. Geophys. Res.*, 112,  
935 D19306, doi: 10.1029/2006JD007308, 2007.

936 Smit, H. G. J. and the ASOPOS panel (Assessment of Standard Operating Procedures for  
937 Ozonesondes): Quality assurance and quality control for ozonesonde measurements in GAW,  
938 World Meteorological Organization, GAW Report #201, Geneva, Switzerland, 2014. available at:  
939 [http://www.wmo.int/pages/prog/arep/gaw/documents/FINAL\\_GAW\\_201\\_Oct\\_2014.pdf](http://www.wmo.int/pages/prog/arep/gaw/documents/FINAL_GAW_201_Oct_2014.pdf).

940 Smit, H. G. J., and the O3S-DQA-Panel (Ozone Sonde Data Quality Assessment): Guidelines for  
941 homogenization of ozonesonde data, SI2N/O3S-DQA activity as part of “Past changes in the  
942 vertical distribution of ozone assessment”, 2012. available at: [http://www-das.uwyo.edu/%7Edehshler/NDACC\\_O3Sondes/O3s\\_DQA/O3S-DQA-Guidelines%20Homogenization-V2-19November2012.pdf](http://www-das.uwyo.edu/%7Edehshler/NDACC_O3Sondes/O3s_DQA/O3S-DQA-Guidelines%20Homogenization-V2-19November2012.pdf)

945 Stauffer, J., J. Staehelin, R. Stübi, T. Peter, F. Tummon, and V. Thouret: Trajectory matching of  
946 ozonesondes and MOZAIC measurements in the UTLS – Part 1: Method description and  
947 application at Payerne, Switzerland, *Atmos. Meas. Tech.*, 6, 3393-3406, doi:10.5194/amt-6-3393-  
948 2013, 2013.

949 Stauffer, J., J. Staehelin, R. Stübi, T. Peter, F. Tummon, and V. Thouret: Trajectory matching of  
950 ozonesondes and MOZAIC measurements in the UTLS – Part 2: Application to the global  
951 ozonesonde network, *Atmos. Meas. Tech.*, 7, 241-266, doi:10.5194/amt-7-241-2014, 2014.

952 Stähelin, J., N. R. P. Harris, C. Appenzeller, and J. Eberhard: Ozone trends: a review, *Rev. Geophys.*,  
953 32 (2), 231-290, 2001.

954 Stein, A.F., D. Lamb, and R.R. Draxler: Incorporation of detailed chemistry into a three dimensional  
955 Lagrangian-Eulerian hybrid model: Application to regional tropospheric ozone, *Atmos. Environ.*,  
956 34, 4361-4372, 2000.

957 Stübi, R., G. Levrat, B. Hoegger, P. Viatte, J. Staehelin, and F. J. Schmidlin: Inflight comparison of  
958 Brewer-Mast and electrochemical concentration cell ozonesondes, *J. Geophys. Res.*, 113, D13302,  
959 doi: 10.1029/2007JD009091, 2008.

960 Tarasick, D. W., Davies, J., Smit, H. G. J., and Oltmans, S. J.: A re-evaluated Canadian ozonesonde  
961 record: measurements of the vertical distribution of ozone over Canada from 1966 to 2013,  
962 *Atmos. Meas. Tech.*, 9, 195-214, doi:10.5194/amt-9-195-2016, 2016.

963 Thornton, D. C. and N. Niazy: Effects of solution mass transport on the ECC ozonesonde background  
964 current, *Geophys. Res. Lett.*, 10, 148-151, 1983.

965 Thornton, D. C. and N. Niazy: Source of background current in ECC ozondesonde: Implication for  
966 total ozone measurements, *J. Geophys. Res.*, 87, 11, 8943-8950, 1982.

967 Thouret, V., Cammas, J.-P., Sauvage, B., Athier, G., Zbinden, R., Nédélec, P., Simon, P., and  
968 Karcher, F.: Tropopause referenced ozone climatology and inter-annual variability (1994–2003)  
969 from the MOZAIC programme, *Atmos. Chem. Phys.*, 6, 1033-1051, doi:10.5194/acp-6-1033-2006,  
970 2006.

971 Thouret, V., A. Marenco, J. A. Logan, P. Nedelev, and C. Grouhel: Comparisons of ozone  
972 measurements from the MOZAIC airborne program and the ozone sounding net-work at eight  
973 locations, *J. Geophys. Res.* 103, 25,695-25,720, doi: 10.1029/98JD02243, 1998.



974 Vömel, H. and Diaz, K.: Ozone sonde cell current measurements and implications for observations of  
975 near-zero ozone concentrations in the tropical upper troposphere, *Atmos. Meas. Tech.*, 3, 495–505,  
976 doi:10.5194/amt-3-495-2010, 2010.

977 WMO: *SPARC-IOC-GAW Assessment of Trends in the Vertical Distribution of Ozone*, SPARC report  
978 No.1, WMO Global Ozone Research and Monitoring Project, Report No. 43, Geneva,  
979 Switzerland, May 1998.

980 WMO: *Scientific Assessment of Ozone Depletion: 2010*, Global Ozone Research and Monitoring  
981 Project-Report No. 52, 516 pp., Geneva, Switzerland, 2010.

982 WMO: *Scientific Assessment of Ozone Depletion: 2014*, Global Ozone Research and Monitoring  
983 Project-Report No. 55, 416 pp., Geneva, Switzerland, 2014.

984

985



986      **Table 1.** Datasets used in the analysis giving experiment or location, years of the comparisons,  
 987      location latitude and longitude, ozonesonde and solution strengths compared, number of comparisons,  
 988      sampling frequency of the data (Hz), and the platform. The multi-sonde platforms contained from 4 to  
 989      12 ozonesondes.  
 990

Location	Dates	Lat.	Long.	Provider-Concen.	No.	Freq	Platform/
JOSIE09	1996-2000	50.9	-6.4	EN-0.5	EN-1.0	3	1
				SP-0.5	SP-1.0	3	
				SP-1.0	EN-1.0	7	
				SP-0.5	EN-0.5	5	
				SP-1.0	EN-0.5	3	
BESOS	April 2004	41.3	105.7	EN-0.5	EN-1.0	9	0.5
				SP-0.5	SP-1.0	9	
				SP-1.0	EN-1.0	9	
				SP-0.5	EN-0.5	9	
				SP-1.0	EN-0.5	9	
Payerne	2002-2003	46.8	-6.9	En-0.5	EN-1.0	48	0.15
				SP-1.0	EN-0.5	26	Dual-sonde
McMurdo	1996-2006	-77.8	166.7	EN-0.5	EN-1.0	18	0.15
Sodankylä	1995-2002	67.4	-26.6	EN-0.5	EN-1.0	4	1
				SP-1.0	EN-1.0	8	Multi- / Dual-
				SP-1.0	EN-0.5	5	sondes
Wallop I.	1995-2002	37.8	75.5	SP-0.5	SP-1.0	16	1
Laramie	1996	41.1	105.6	EN-0.5	EN-1.0	6	Multi-sonde
Total				EN-0.5	EN-1.0	88	KI conc. diff.
				SP-0.5	SP-1.0	28	KI conc. diff.
				SP-1.0	EN-1.0	24	Sonde diff.
				SP-0.5	EN-0.5	14	Sonde diff.
				SP-1.0	EN-0.5	43	Recommended

991  
 992



993      **Table 2.** Mean and standard deviations of the various comparison measurements. The mean ratio is  
 994      equivalent to the slope of a linear fit to the data which passes through the origin. For the datasets with  
 995      the most data and the most varied comparisons the means and standard deviations are given for the  
 996      pressure intervals indicated at the top. For the other datasets the means and standard deviations are  
 997      given for all the data without regard to pressure.  
 998

Source	Sonde/KI	From	To	999>p>500	500>p>100	100>p>30	30>p
JOSIE09	EN	1.0%	0.5%	0.96±0.02	0.95±0.04	0.94±0.05	0.91±0.07
BESOS	EN			0.95±0.07	0.95±0.03	0.95±0.04	0.94±0.01
Payerne	EN			0.97±0.84	0.97±0.05	0.96±0.03	0.94±0.04
McMurdo	EN			0.97±0.04	0.96±0.06	0.96±0.09	0.92±0.06
Sodankylä	EN			0.93±0.03	All data		
Wallops I.	EN			0.92±0.06	All data		
Laramie	EN			0.96±0.04	All data		
JOSIE09	SP	1.0%	0.5%	0.97±0.02	0.97±0.02	0.98±0.03	0.93±0.06
BESOS	SP			0.97±0.02	0.96±0.02	0.95±0.02	0.93±0.02
Wallops I.	SP			0.94±0.06	All data		
JOSIE09	1.0%	SP	EN	0.96±0.02	0.94±0.05	0.94±0.12	0.93±0.05
BESOS	1.0%			0.97±0.13	0.97±0.03	0.96±0.04	0.96±0.02
Sodankylä	1.0%			0.95±0.03	All data		
JOSIE09	0.5%	SP	EN	0.96±0.03	0.95±0.04	0.96±0.06	0.94±0.05
BESOS	0.5%			1.00±0.07	0.98±0.03	0.96±0.03	0.96±0.02
JOSIE09		SP-1.0	EN-0.5	1.01±0.04	0.99±0.03	1.00±0.04	0.98±0.03
BESOS				1.02±0.13	1.03±0.03	1.01±0.03	1.02±0.02
Payerne				1.03±0.46	1.00±0.06	1.00±0.04	1.01±0.03
Sodankylä				1.02±0.03	All data		

999  
 1000



1001  
 1002  
 1003  
 1004  
 1005  
 1006  
 1007

**Table 3.** Transfer function parameters summary. The second and third columns are for  $p \geq 30$  hPa providing the ratio and number of data points. Columns 4 – 7 are for  $p < 30$  hPa, providing the slope of a linear fit in  $\log_{10}(p)$ , the offset adjusted to match the ratio at 30 hPa, the offset without constraint to the data below and number of data points. The offset is value of the ratio at  $p=1$  hPa. The final column is the number of dual sonde measurements for each data set for each application.

Dataset	Ratio, $p > 30$	$N(p > 30)$	Slope	Offset	Offset no	N	No.
EN 0.5% to EN 1.0% - Compare Solution Strengths							
JOSIE09	0.943±0.056	1918	-0.176	1.203	1.052	949	3
BESOS	0.951±0.028	5003	0.041	0.981	0.882	1854	9
Payerne	0.965±0.546	34855	0.031	0.920	0.910	14744	48
Sodankylä	0.941±0.027	2291	0.109	0.780	0.762	524	4
McMurdo	0.977±0.124	15030	0.118	0.802	0.785	4197	18
Laramie	0.974±0.044	1290	0.063	0.882	0.848	378	6
Weighted	0.966±0.142	60387	0.041	0.904	0.886	22676	88
SP 0.5% to SP 1.0% - Compare Solution Strengths							
JOSIE09	0.955±0.129	1919	-0.164	1.198	1.051	949	3
BESOS	0.975±0.105	5005	0.014	0.954	0.914	1854	9
Wallop I.	0.937±0.065	10123	0.052	0.860	0.865	2083	16
Weighted	0.950±0.176	17047	-0.004	0.962	0.919	4886	28
SP 1.0% to EN 1.0% - Compare Sonde Providers							
JOSIE09	0.945±0.0074	4475	0.133	0.749	0.744	2217	7
BESOS	0.959±0.061	5005	0.145	0.745	0.756	1854	9
Sodankylä	0.963±0.026	4041	0.112	0.798	0.784	961	8
Weighted	0.956±0.094	13521	0.133	0.757	0.756	5032	24
SP 0.5% to EN 0.5% - Compare Sonde Providers							
JOSIE09	0.954±0.054	3193	0.179	0.690	0.680	1587	5
BESOS	0.977±0.0027	5003	0.119	0.801	0.786	1854	9
Weighted	0.968±0.040	8196	0.147	0.750	0.737	3441	14
SP 1.0% to EN 0.5% - The Provider Recommendations							
JOSIE09	0.998±0.055	1919	0.880	-0.301	0.142	949	3
BESOS	1.009±0.068	5004	0.112	0.842	0.864	1854	9
Payerne	1.008±0.251	17123	0.065	0.912	0.927	7069	26
Sodankylä	1.023±0.027	2462	0.003	1.019	1.015	642	5
Weighted	1.009±0.091	26508	0.143	0.797	0.850	10514	43

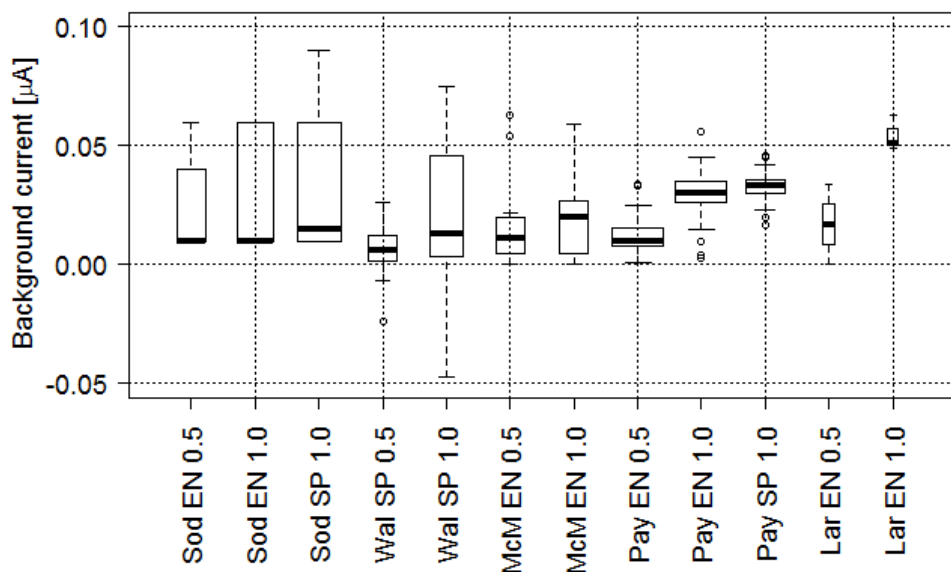
1008  
 1009



1010 **Table 4.** Ratios of total column ozone at Nairobi, Kenya, measured either with the OMI satellite  
 1011 instrument or a Dobson Spectrophotometer, compared to EN ozonesondes using 1.0% and 0.5% KI  
 1012 concentrations. The ratios are also shown after correction of the EN-1.0% to EN-0.5% ( $OZ_{conc}$ ). Two  
 1013 approaches for the residual ozone column above the balloon burst are given: constant mixing ratio  
 1014 (MR) and using climatology [McPeters and Labow, 2012], the WMO recommendation.  
 1015

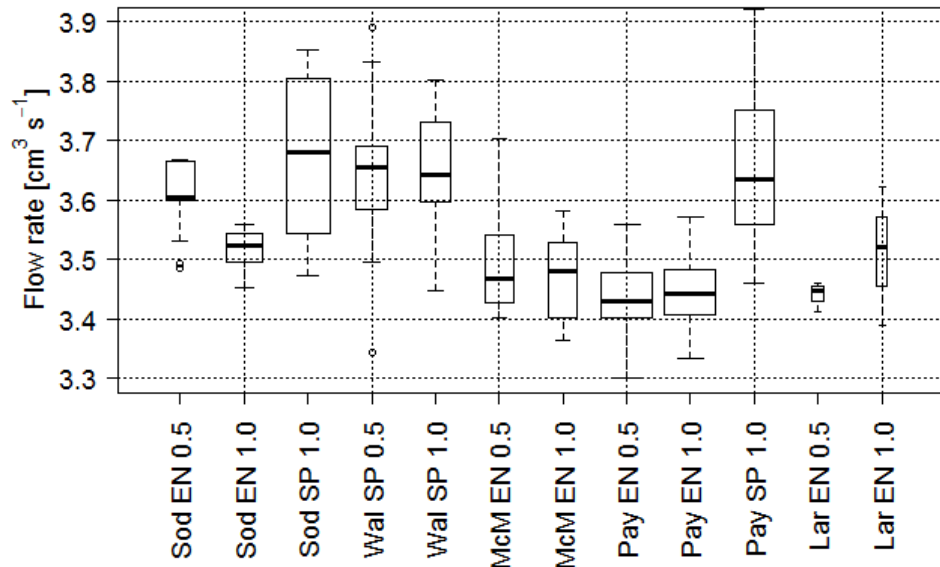
Ratios	OMI / EN-1.0%	OMI / $OZ_{conc}$	OMI / EN-0.5%	Dobson/ EN-1.0%	Dobson / $OZ_{conc}$	Dobson / EN-0.5%
Medians	0.93	0.98	0.96	0.92	0.96	0.94
Constant MR	$\pm 0.04$	$\pm 0.04$	$\pm 0.04$	$\pm 0.05$	$\pm 0.05$	$\pm 0.05$
Medians	0.95	0.98	0.94	0.92	0.96	0.92
Climatology	$\pm 0.03$	$\pm 0.03$	$\pm 0.03$	$\pm 0.04$	$\pm 0.04$	$\pm 0.05$

1016  
 1017  
 1018  
 1019  
 1020  
 1021



1022  
 1023 **Figure 1.** Boxplot of the background current ( $\mu$ A) measured at the five stations which flew a  
 1024 number of dual or multi ozonesonde gondolas: Sodankylä (Sod), Wallops Island (Wal),  
 1025 McMurdo Station (McM), Payerne (Pay), and Laramie (Lar). Following the station location,  
 1026 the ozonesonde manufacturer is identified (EN or SP) and then the KI solution concentration  
 1027 (0.5% or 1.0%). Medians are the thick black segments, the inter-quartile range the box height,  
 1028 1.5 times the inter-quartile range the whiskers, outliers denoted as circles, the square root of  
 1029 the number of measurements is reflected in the box width. A value of 0.03  $\mu$ A corresponds to  
 1030 0.1 mPa of ozone.

1031



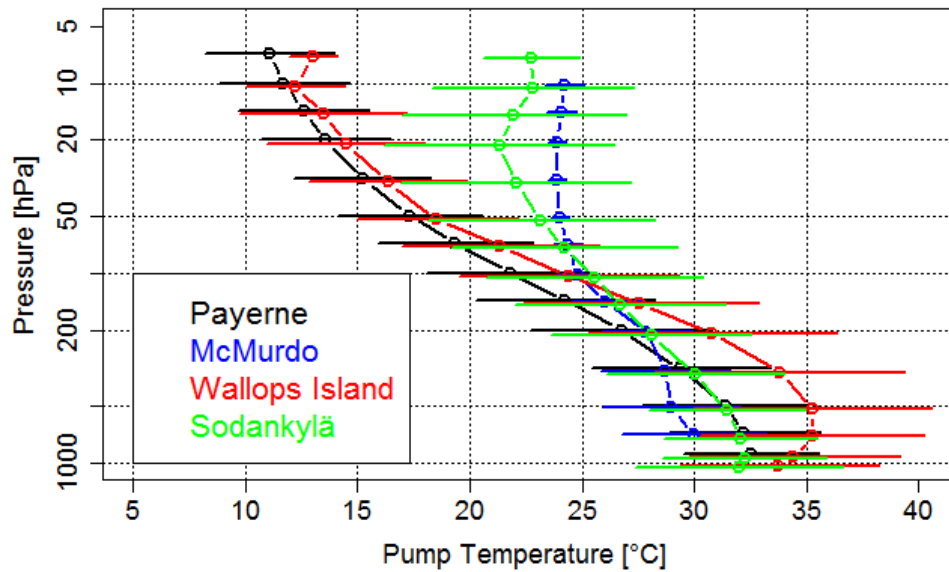
1032

1033 **Figure 2.** Ozonesonde pump flow rates (cm<sup>3</sup> s<sup>-1</sup>) measured at the different stations, following  
1034 the nomenclature of Figure 1 for the station and ozonesonde.

1035



1036

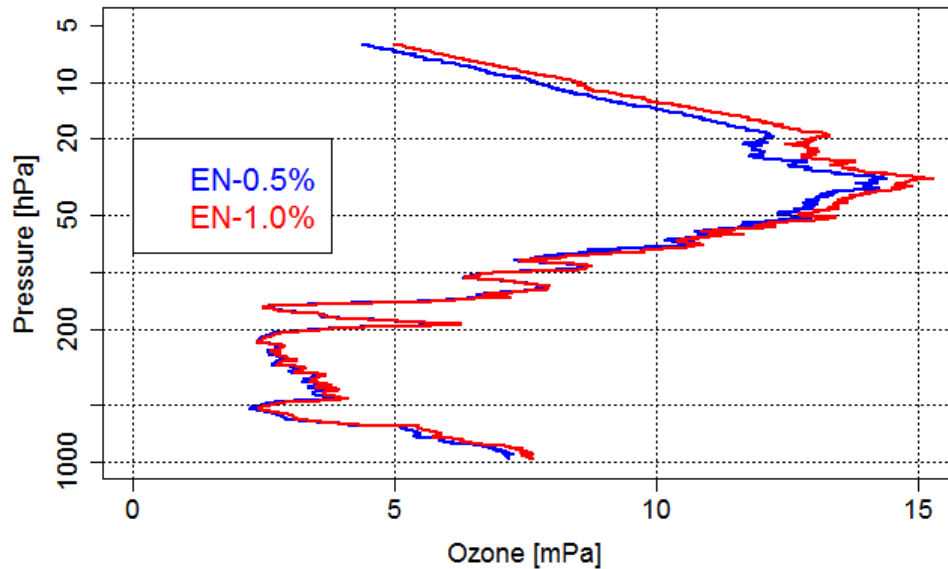


1037

1038 **Figure 3.** Mean profile of the measured pump temperature for the different dual flight data  
1039 sets. The higher pump temperature at the upper part of the profiles for the McMurdo and  
1040 Sodankylä stations is due to a heat source to avoid freezing of the solution. Error bars are one  
1041 standard deviation of the measurements.

1042

1043



1044

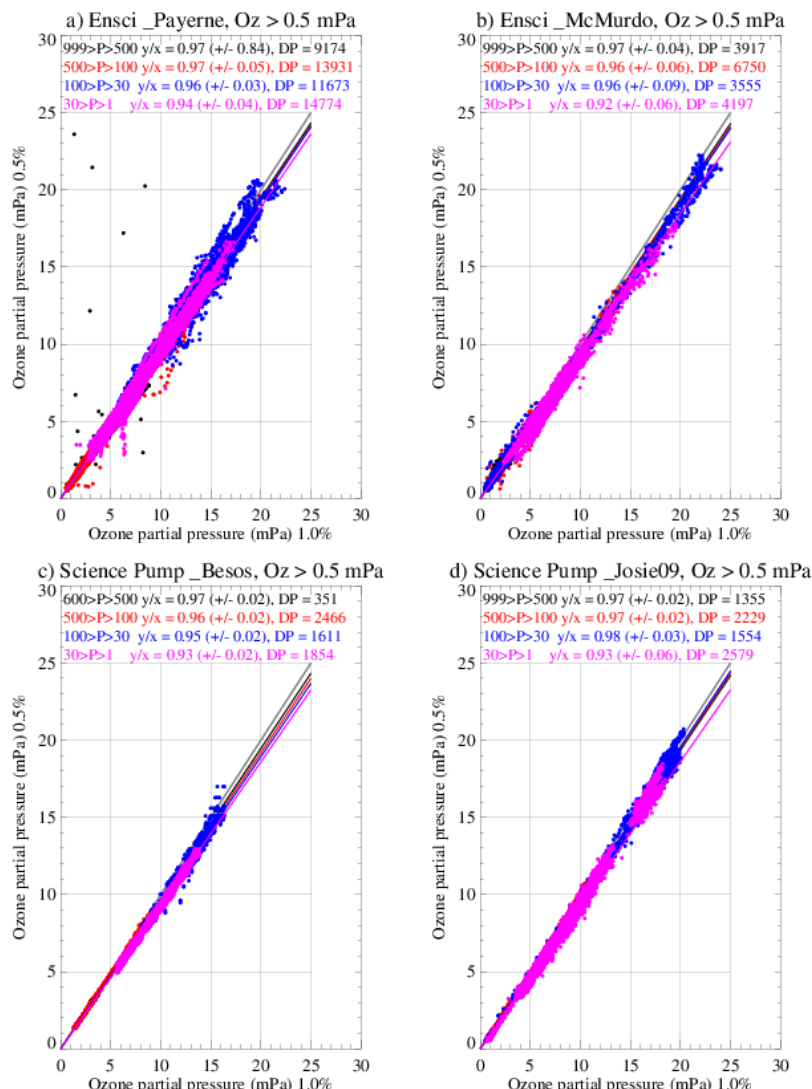
1045 **Figure 4.** Example of the results of a dual flight profile from Payerne. The only difference  
1046 between the ozonesondes is the KI solution concentration.

1047

1048



1049



1050

1051 **Figure 5.** Scatter plots of ozone partial pressures measured with KI concentrations of 1.0%  
 1052 (x-axis) and 0.5% (ordinate-axis) using EN ozonesondes flown from a) Payerne, b) McMurdo  
 1053 Station, and with SP ozonesondes from c) BESOS, and d) JOSIE09. The data are subdivided  
 1054 into four pressure intervals and averages and standard deviations of the ratios of y:x are listed  
 1055 on the panels along with the number of measurements. Only ozone measurements above 0.5  
 1056 mPa are included. At  $p \geq 30$  hPa there is little variation in the ratios either by pressure  
 1057 interval, location, or ozonesonde type. At  $p < 30$  hPa ratios are decreasing. The 1:1 line is  
 1058 shown in gray.

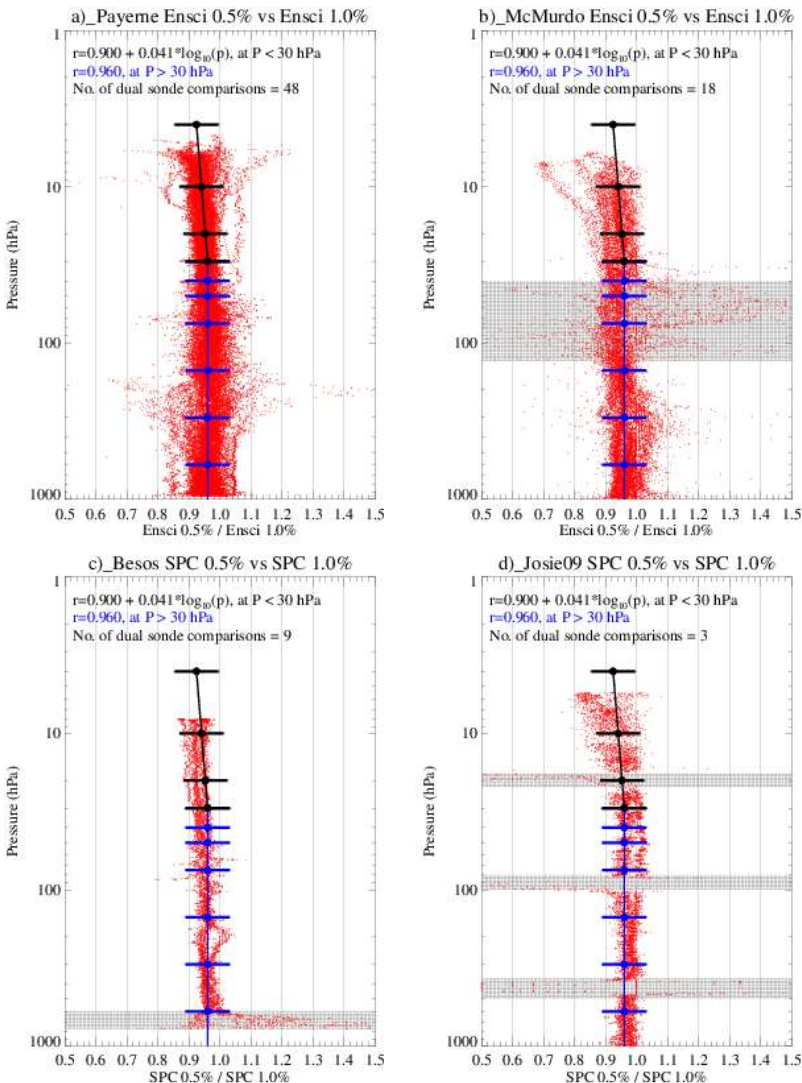


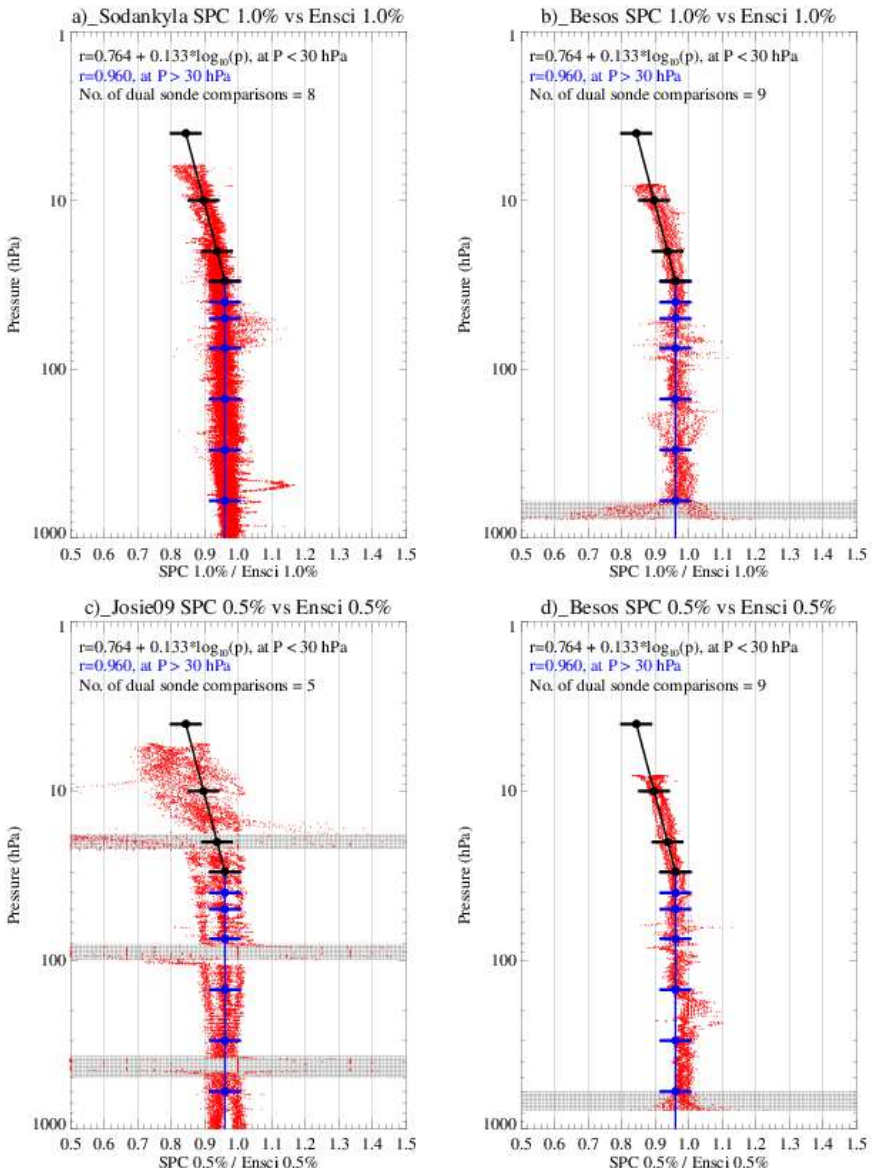
1059

1060

1061 **Figure 6.** Vertical profiles of ratios of ozone partial pressure using ozonesondes with different  
 1062 KI concentrations (0.5%, 1.0%) in ozonesondes of the same manufacturer, EN or SP. a)  
 1063 Payerne - EN, b) McMurdo -EN, c) BESOS – SP, and d) JOSIE09 – SP. The hashed areas  
 1064 are regions of low ozone in: ozone hole measurements, McMurdo; tests in the laboratory,  
 1065 JOSIE09; or during initial problems with the BESOS data system at the lowest altitudes.

1066



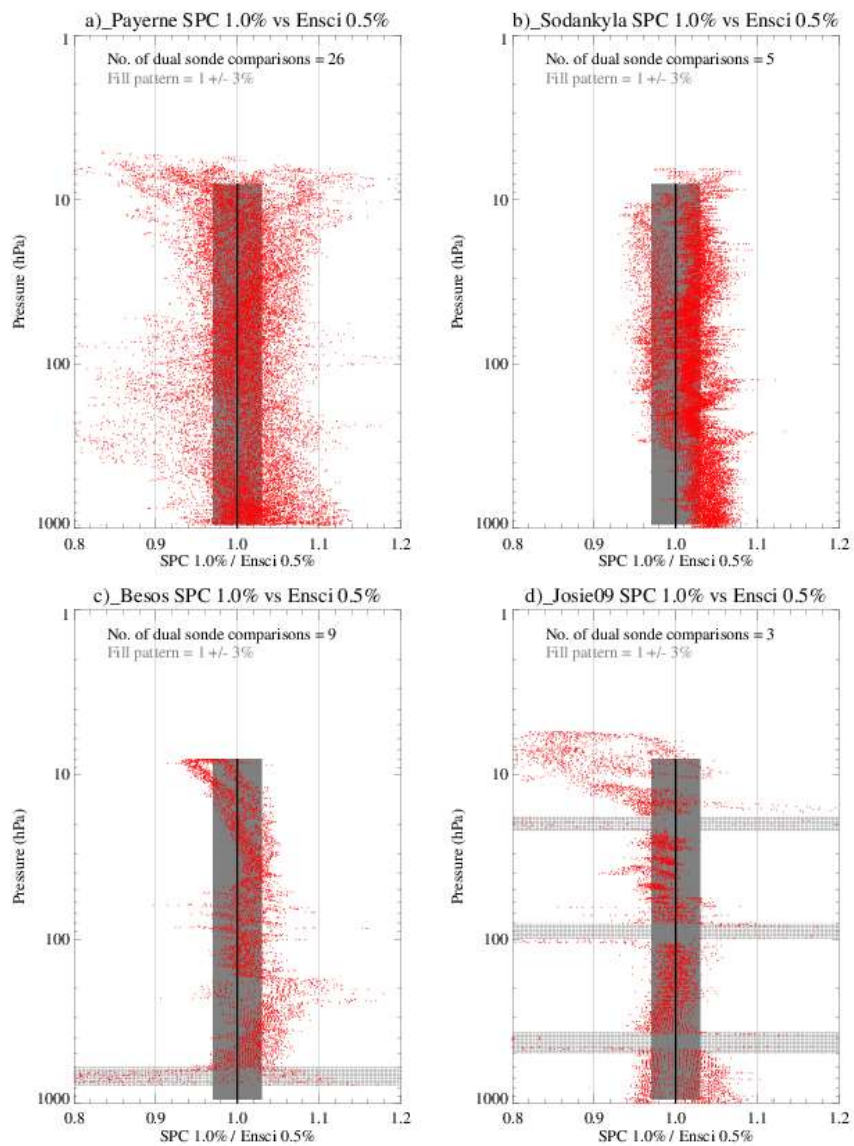


1067

1068 **Figure 7.** Vertical profiles of ratios of ozone partial pressure using ozonesondes of different  
 1069 manufacturers (SP, EN) with the same KI concentrations in both ozonesondes, either 1.0% (top  
 1070 two panels) or 0.5% (bottom two panels). a) Sodankylä – 1.0%, b) BESOS – 1.0%, c)  
 1071 JOSIE09 – 0.5%, d) BESOS – 0.5%. The hashed areas denote regions of low ozone in tests in  
 1072 the laboratory during JOSIE09, or during initial problems with the BESOS data system at the  
 1073 lowest altitudes.



1074



1075

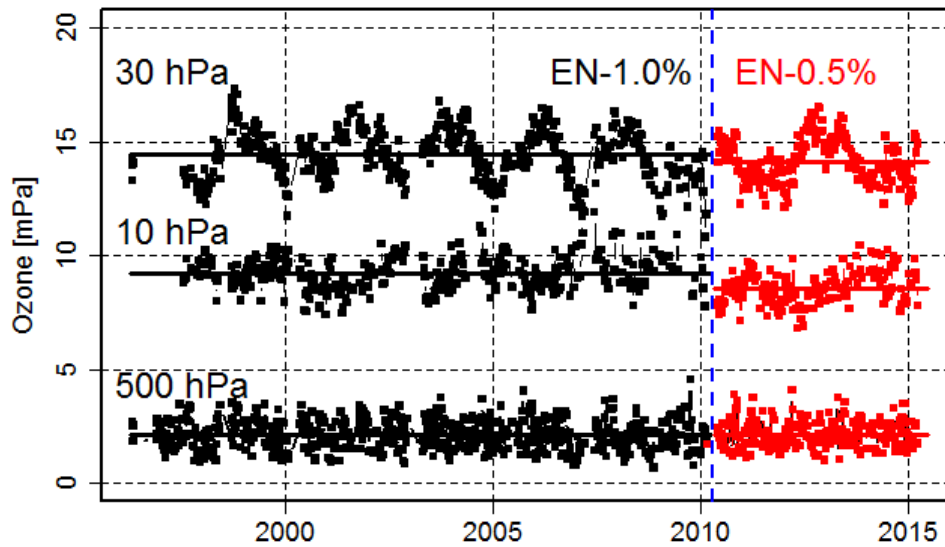
1076 **Figure 8.** Ratios of SP-1.0% with EN-0.5% ozonesondes. The measurements are from a)  
1077 Payerne, b) Sodankylä, c) BESOS, and d) JOSIE 2009. The filled regions represent 3%  
1078 around 1.0. The hashed areas are as before to indicate regions of low ozone concentration  
1079 during tests in JOSIE 2009 or difficulty with the data system in BESOS.

1080



1081

1082



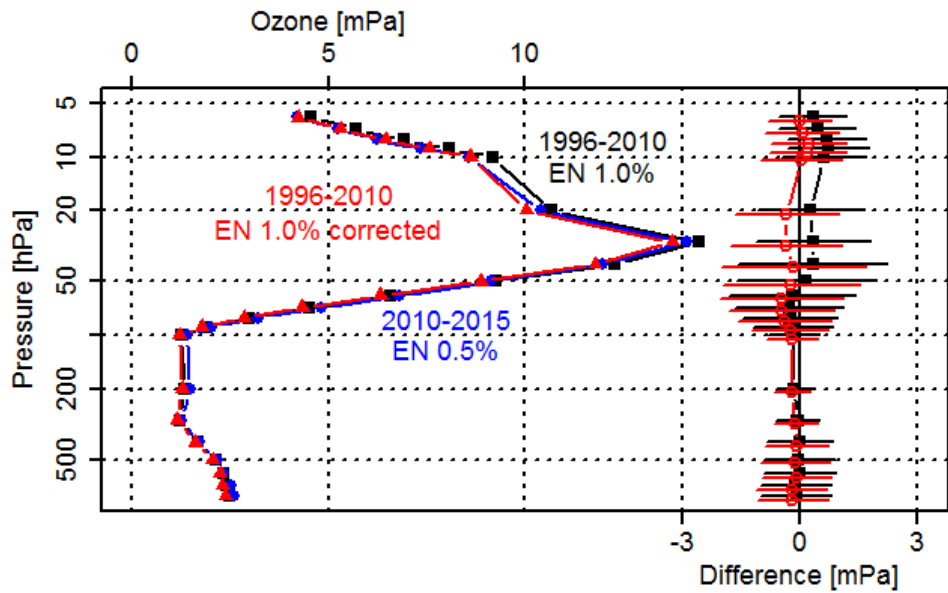
1083

1084 **Figure 9.** Ozone time series from the Nairobi station at three pressure levels: 500, 30 and 10  
1085 hPa. The black symbols correspond to the data from 1996 - 2010 (EN-1.0% solution) and the  
1086 red symbols from 2010 onwards (EN-0.5%). The horizontal segments are the mean values  
1087 over the two periods. No corrections to the EN-1.0% data have been made for this figure.

1088

1089

1090



1091  
1092

1093 **Figure 10.** On the left (upper scale), mean ozone profile for the EN-1.0% period in black,  
1094 EN-0.5% period in blue and corrected EN-1.0% profile using  $OZ_{conc}$  in red for the Nairobi  
1095 data set. On the right (lower scale), the difference between the mean (1996-2010) ozone  
1096 profiles and the mean (2010-2015) profiles before (after), black (red) correction for the  
1097 change of solution concentration that occurred in 2010. A small offset of the pressure scale is  
1098 used to avoid overlapping error bars.  
1099  
1100  
1101